Biomedicine & Pharmacotherapy 155 (2022) 113773

Contents lists available at ScienceDirect

Biomedicine & Pharmacotherapy

journal homepage: www.elsevier.com/locate/biopha

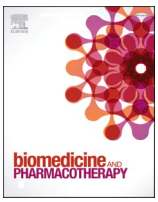

Anti-influenza A virus activity by *Agrimonia pilosa* and *Galla rhois* extract mixture

Yong-Hyun Joo [a], Yeong-Geun Lee [b], Younghyun Lim [a], Hoyeon Jeon [a], In-Gu Lee [a], Yong-Bin Cho [a], So-Hee Hong [c], Eui Ho Kim [d], Soon Ho Choi [e], Jung-Woong Kim [a,*], Se Chan Kang [b,**], Young-Jin Seo [a,*]

[a] Department of Life Science, Chung-Ang University, Seoul, Republic of Korea
[b] Department of Oriental Medicine Biotechnology, College of Life Science, Kyung Hee University, Yongin, Republic of Korea
[c] Department of Microbiology, College of Medicine, Ewha Womans University, Seoul, Republic of Korea
[d] Viral Immunology Laboratory, Institut Pasteur Korea, Seongnam, Republic of Korea
[e] Research Institute, APRG Inc., Yongin, Gyeonggi-do, Republic of Korea

ARTICLE INFO

Keywords:
Antiviral drug
Influenza A virus
APRG64
Apigenin

ABSTRACT

Influenza A virus (IAV) continues to threaten human health. To date, two classes of antiviral drugs have been approved to treat IAV infection, but the continuous emergence of the drug-resistant IAV mutant reinforces the need to develop new antiviral drugs. In this study, we aimed to investigate the anti-IAV activity of an aqueous mixture of *Agrimonia pilosa* and *Galla rhois* extracts (APRG64). We demonstrated that APRG64 significantly reduced the IAV-induced cytopathic effect, the transcription/expression of viral proteins, and the production of infectious viral particles. Among nine major components of APRG64, apigenin was identified as the main ingredient responsible for the anti-IAV activity. Interestingly, APRG64 and apigenin inhibited the cell attachment and entry of virus and polymerase activity. Importantly, intranasal administration of APRG64 or apigenin strongly reduced viral loads in the lungs of IAV-infected mice. Furthermore, oral administration of APRG64 significantly reduced the level of viral RNAs and the expression level of pro-inflammatory cytokines in the lungs, which protected mice from IAV-induced mortality. In conclusion, APRG64 could be an attractive antiviral drug to treat IAV infection.

1. Introduction

The influenza virus is a major infectious pathogen causing acute respiratory disease. Due to its high transmissibility and mortality, the influenza virus imposes a huge global burden on public health and the economy [1,2]. The World Health Organization (WHO) estimates that seasonal flu causes 290,000–650,000 deaths annually [3]. Influenza A virus (IAV) is known to have greater potential to cause deadly pandemic outbreaks than influenza B or C viruses [1]. For example, the 1918 Spanish flu and 2009 swine flu pandemics have resulted in substantial morbidity and mortality [4].

Under the continuing threat of IAV, annual vaccination is the most effective strategy to prevent IAV infection [5,6]. However, the effectiveness of the IAV vaccine is frequently compromised due to antigenic drifts or shifts caused by mutations in the viral RNA genome. Subsequently, new IAV variants often emerge that are capable of escaping from vaccine-induced immunity [7]. To treat IAV-infected patients, antiviral drugs, such as the neuraminidase inhibitor oseltamivir and the IAV M2 protein inhibitor rimantadine, are clinically used to alleviate symptoms and related complications [8]. Despite the effectiveness of

Abbreviations: AP, *Agrimonia pilosa*; APRG64, 50% ethanol aqueous extract mixture of *Agrimonia pilosa* and *Galla rhois* in a 6:4 ratio; CPE, cytopathic effect; C_t, cycle threshold; c.c., column chromatography; dpi, days post-infection; FBS, fetal bovine serum; hpi, hours post-infection; IAV, influenza virus type A; MDCK, Madin-Darby canine kidney; MEM, minimum essential medium; mpk, milligram per kilogram; ODS, octadecyl silica gel; pfu, plaque-forming units; RG, *Galla rhois*; SiO_2, silica gel.

* Correspondence to: Department of Life Science, Chung-Ang University, 84 Heukseok-ro, Dongjak-gu, Seoul 06974, Republic of Korea.
** Correspondence to: Department of Oriental Medicine Biotechnology, College of Life sciences, Kyung Hee University, 1732 Deogyeong-daero, Giheung-gu, Yongin, Gyeonggi 17104, Republic of Korea.
E-mail addresses: jungkim@cau.ac.kr (J.-W. Kim), sckang@khu.ac.kr (S.C. Kang), yjseo@cau.ac.kr (Y.-J. Seo).

https://doi.org/10.1016/j.biopha.2022.113773
Received 30 May 2022; Received in revised form 19 September 2022; Accepted 27 September 2022
Available online 30 September 2022

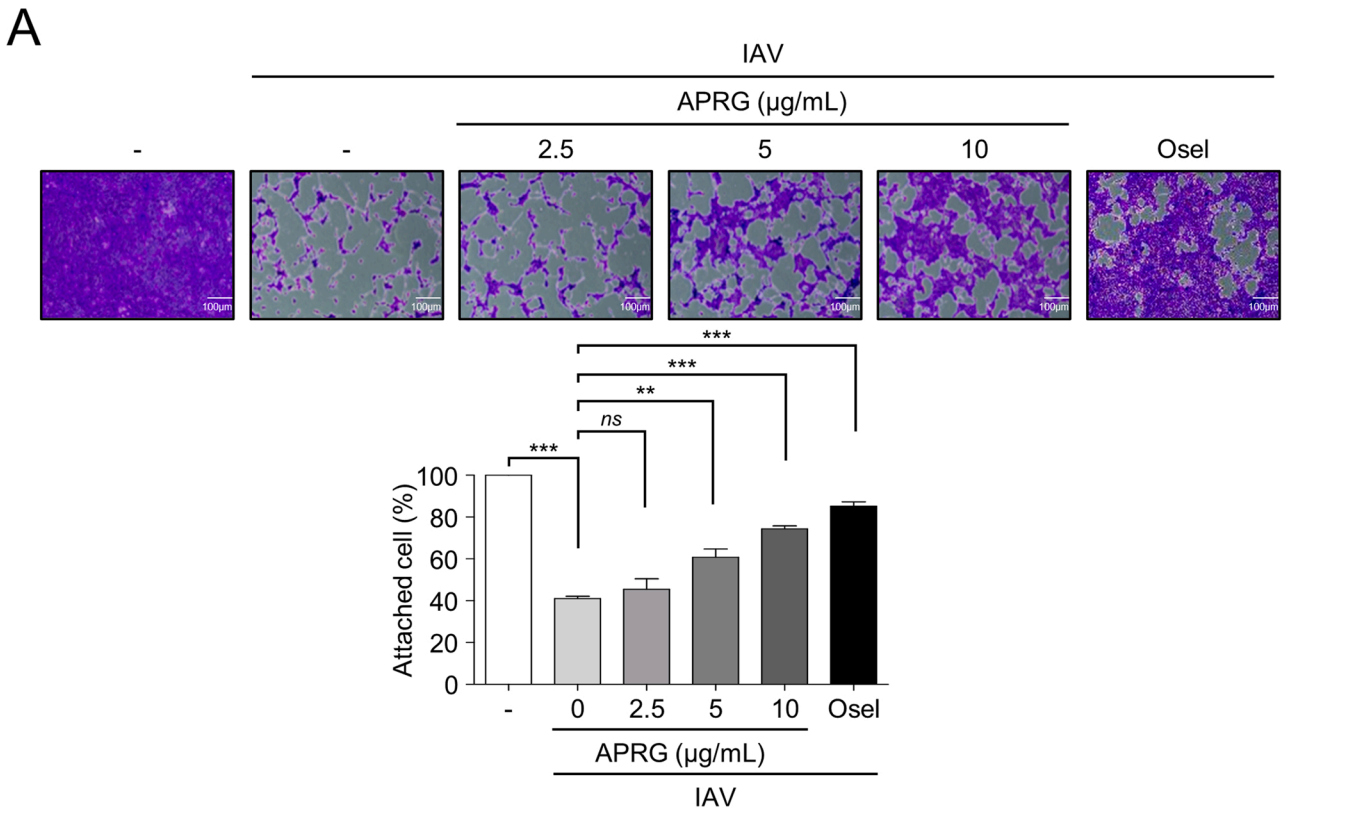

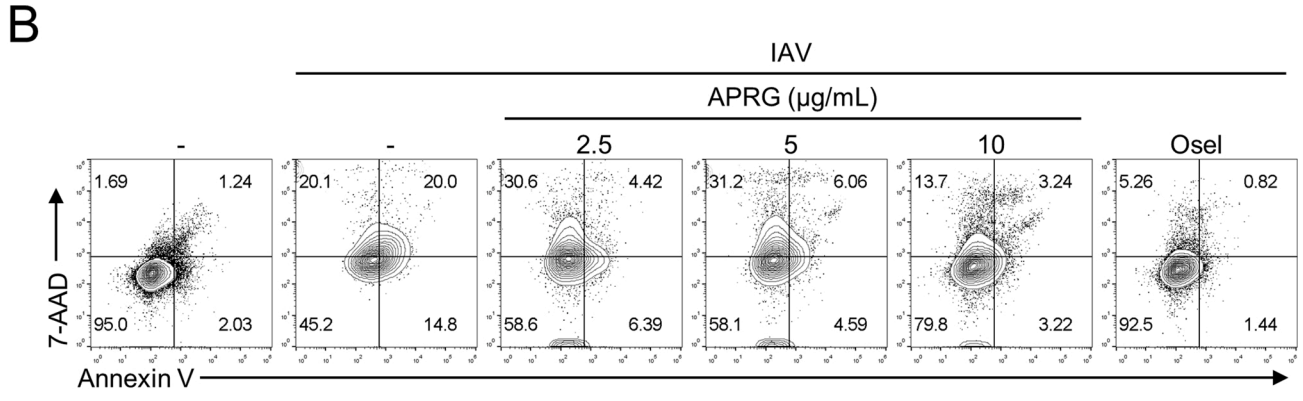

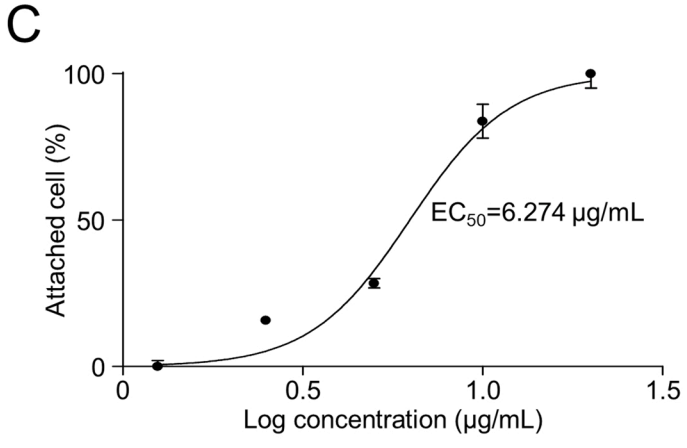

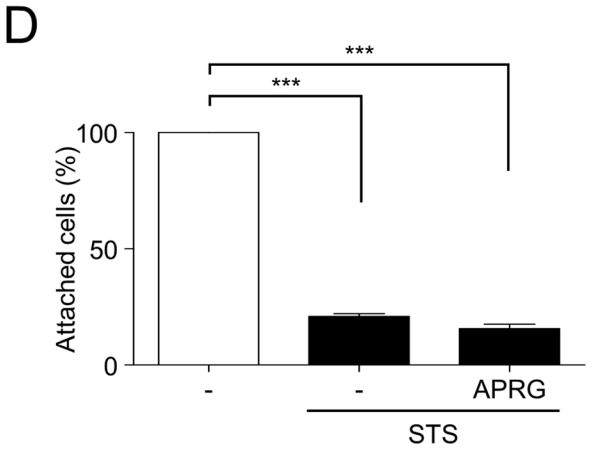

(caption on next page)

Fig. 1. The inhibitory effect of APRG64 on IAV-induced CPEs. (A) MDCK cells were infected with IAV at a multiplicity of infection (MOI) of 0.1 for 1 h, then untreated or treated with APRG64 (2.5, 5 or 10 μg/mL) or 10 μg/mL of oseltamivir phosphate for 24 h. Cells were stained with 1 % crystal violet solution to analyze the percentage of attached cells. Representative images and the percentage of attached cells are presented. (**B**) MDCK cells were infected with IAV at an MOI of 0.1 for 1 h, then treated with APRG64 (2.5, 5 or 10 μg/mL) or oseltamivir phosphate (10 μg/mL). After 12 hpi, cells were stained with 7-AAD and Annexin V to analyze apoptosis by flow cytometry. (**C**) MDCK cells were infected with IAV at an MOI of 0.1 for 1 h, then treated with 0, 1.25, 2.50, 5.00, 10.00, or 20.00 μg/mL of APRG64. At 24 hpi, cells were stained with 1% crystal violet solution to determine the EC_{50} of APRG64. (**D**) MDCK cells were untreated or treated with 200 nM of staurosporine (STS) in the presence or absence of APRG64 (10 μg/mL), after which cell viability was analyzed using 1 % crystal violet staining. Images were processed by ImageJ software to quantify attached cells on the plate. Water was used as solvent control for APRG64. All graphs represent the average of three replicates. Significance was determined by Student's *t*-test. * , $p \leq 0.05$; **, $p \leq 0.01$; *** , $p \leq 0.001$. APRG: APRG64; Osel: Oseltamivir phosphate.

these drugs at reducing influenza-related morbidity and mortality, the emergence of the drug-resistant variants poses a critical limitation to their application. Antiviral drug-resistant variants have long been associated with an increasing rate of seasonal influenza, probably due to the widespread or indiscriminate use of antiviral drugs [9]. Thus, the development of new antiviral drugs alongside the evolution of IAV is essential to control IAV infections.

Agrimonia pilosa Ledeb. (Rosaceae) (AP), which belongs to the Rosaceae family, reportedly possesses diverse biological activities, such as antimicrobial [10], antihemostatic [11], antitumor [12], and antiviral properties [13–16]. *Galla rhois* (Anacardiaceae) (RG), the gall produced by the aphid *Schlechrendalia chineneis* (Bell), reportedly has antidiarrheal [17] and antimicrobial effects [18]. Interestingly, our previous studies showed that an aqueous mixture of AP and RG extracts in a 6:4 ratio (APRG64) exhibited potent antiviral activities against RNA viruses, including hepatitis C virus (HCV) [19] and severe acute respiratory syndrome coronavirus 2 (SARS-CoV-2) [20]. Considering the impact of influenza on public health, we further investigated whether APRG64 also has antiviral activity against IAV infection.

2. Materials and methods

2.1. Plant materials, reagents, and instruments

Dried aerial parts of AP (place of origin: Korea) and RG (place of origin: Korea) were purchased from BioKorea Co., Ltd. (Seoul, Korea). Each sample was identified and authenticated based on its micro- and macroscopic characteristics. Voucher specimens (BMRI-AP-1601 and BMRI-RG-1602) were deposited in the Bio-Medical Research Institute, Kyung Hee University. Extraction process and validation of each extract was reported in our previous publication [21]. Each sample (20 kg) was extracted with 50 % aqueous ethanol at 80 ± 2 °C for 6 h and filtered. The extracts of AP and RG were concentrated in vacuo. The resultant final product yields of AP and RG were 1.57 and 11.59 kg, respectively. The mixture of AP and RG, APRG64 was composed of the two extracts at a 6:4 ratio. All samples were stored at 4 °C prior to use. Oseltamivir phosphate (Sigma-Aldrich, St. Louis, MO, USA) was used as a positive control.

The silica gel (SiO_2) and the octadecyl silica gel (ODS) resins used for column chromatography (c.c.) were Kieselgel 60 (Merck, Darmstadt, Germany) and LiChroprep RP-18 (40–60 μm; Merck), respectively. Sephadex LH-20 was purchased from Amersham Biosciences (Uppsala, Sweden). Thin-layer chromatography (TLC) was carried out using Kieselgel 60 F_{254} and RP-18 F_{254S} (Merck) TLC plates, and spots were detected using a Spectroline Model ENF-240 C/F ultraviolet (UV) lamp (Spectronics Corp., Westbury, NY, USA) and 10 % sulfuric acid (H_2SO_4) solution. Deuterium solvents were purchased from Merck and Sigma-Aldrich Co., Ltd. Nuclear magnetic resonance (NMR) spectra were recorded on a 600 MHz FT NMR spectrometer (Bruker Avance 600, Rheinstetten, Germany). Infrared (IR) spectra were obtained using a Perkin Elmer Spectrum One FT-IR spectrometer (Buckinghamshire, England). Fast atom bombardment mass spectrometry (FAB/MS) spectra were recorded on a JEOL JMS-700 (Tokyo, Japan). Melting points were obtained using a Fisher-Johns melting point apparatus (Fisher Scientific, Miami, FL, USA) with a microscope; the obtained values were uncorrected.

2.2. Cell and virus

Madin-Darby canine kidney (MDCK) cells were maintained in a humidified incubator at 37 °C in the presence of 5 % CO_2. Cells were cultured in minimum essential medium (MEM, GenDEPOT, Katy, TX, USA) containing 10 % fetal bovine serum (FBS, GenDEPOT) and 1 % penicillin-streptomycin (PS, Welgene, Daegu, Korea). Trypan blue dye solution (Thermo Scientific) was used for the trypan blue exclusion assay. Influenza A/California/07/2009 (H1N1) virus, A/Puerto Rico/8/34 (H1N1, PR8) virus, and A/Aichi/2/68 (H3N2) virus were kindly provided by Dr. Sang-Myeong Lee (Chungbuk National University, Korea). For the infection, MDCK cells were incubated with IAV for 1 h in MEM containing 0.3 % bovine serum albumin (BSA) (Thermo Scientific), and 2 μg/mL of TPCK-treated trypsin (Sigma-Aldrich). Amplification and titration of the virus were performed in accordance with the previously described method [22].

2.3. Cytopathic effect (CPE) assay

The CPE caused by influenza virus infection was visualized by crystal violet staining. Briefly, IAV-infected MDCK cells were untreated or treated with APRG64 for 24 h. Cells were subsequently fixed with 3.5% formaldehyde (Samchun, Seoul, Korea) for 10 min and then stained with a 1% crystal violet solution (Sigma-Aldrich). Each assay was performed at least three independent times in triplicate with similar results.

2.4. Apoptosis analysis

To analyze apoptosis, MDCK cells were stained with 7-AAD and Annexin V conjugated with Allophycocyanin (APC) (BioLegend, San Diego, CA, USA). The data collected on the Attune™ NxT Acoustic Focusing Cytometer (Thermo Scientific) were analyzed by FlowJo software (BD Biosciences, Franklin Lakes, NJ, USA). Each assay was performed three independent times with similar results.

2.5. Real-time quantitative PCR (RT-qPCR)

To extract total RNA from cells, NucleoZOL (Macherey-Nagel, Düren, Germany) was used in accordance with the manufacturer's instructions. Three hundred nanograms of RNA was used to synthesize cDNA using the ReverTraAce qPCR RT kit (Toyobo, Osaka, Japan). Forward (F) and reverse (R) primer sequences for amplification of genes were as follows: viral matrix protein M1, (F) 5′-AAGACCAATCCTGTCACCTCTG-3′ and (R) 5′-CAAAACGTCTACGCTGCAGTCC-3′; viral nucleoprotein (NP), (F) 5′-CCAGATCAGTGTGCAGCCTA-3′ and (R) 5′-CTTCTGGCTTTGCACTTTCC-3′, positive (+) strand of viral M1, (F) 5′-AAGACCAATCCTGTCACCTCTG-3 and (R) 5′-CAAAACGTCTACGCTGCAGTCC-3′; positive strand of viral NP (F) 5′-CCAGATCAGTGTGCAGCCTA-3′ and (R) 5′-CTTCTGGCTTTGCACTTTCC-3′; glyceraldehyde-3-phosphate dehydrogenase (GAPDH) for MDCK, (F) 5′-AACATCATCCCTGCTTCCAC-3′ and (R) 5′-GACCACCTGGTCCTCAGTGT-3′, tumor necrosis factor-alpha (TNF-α) for mouse, (F) 5′-GCCTCTTCTCATTCCTGCTTG-3′ and (R) 5′-CTGATGAGAGGGAGGCCATT-3′, interferon-gamma (IFN-γ) for mouse, (F) 5′-GGCCATCAGCAACAACATAAGCGT-3′, and (R) 5′-TGGGTTGTTGACCTCAAACTTGGC-3′, interleukin-6 (IL-6) for mouse, (F) 5′-ACGGCCTTCCCTACTTCACA-3′ and (R) 5′-CATTTCCACGATTTCCCAGA-3′,

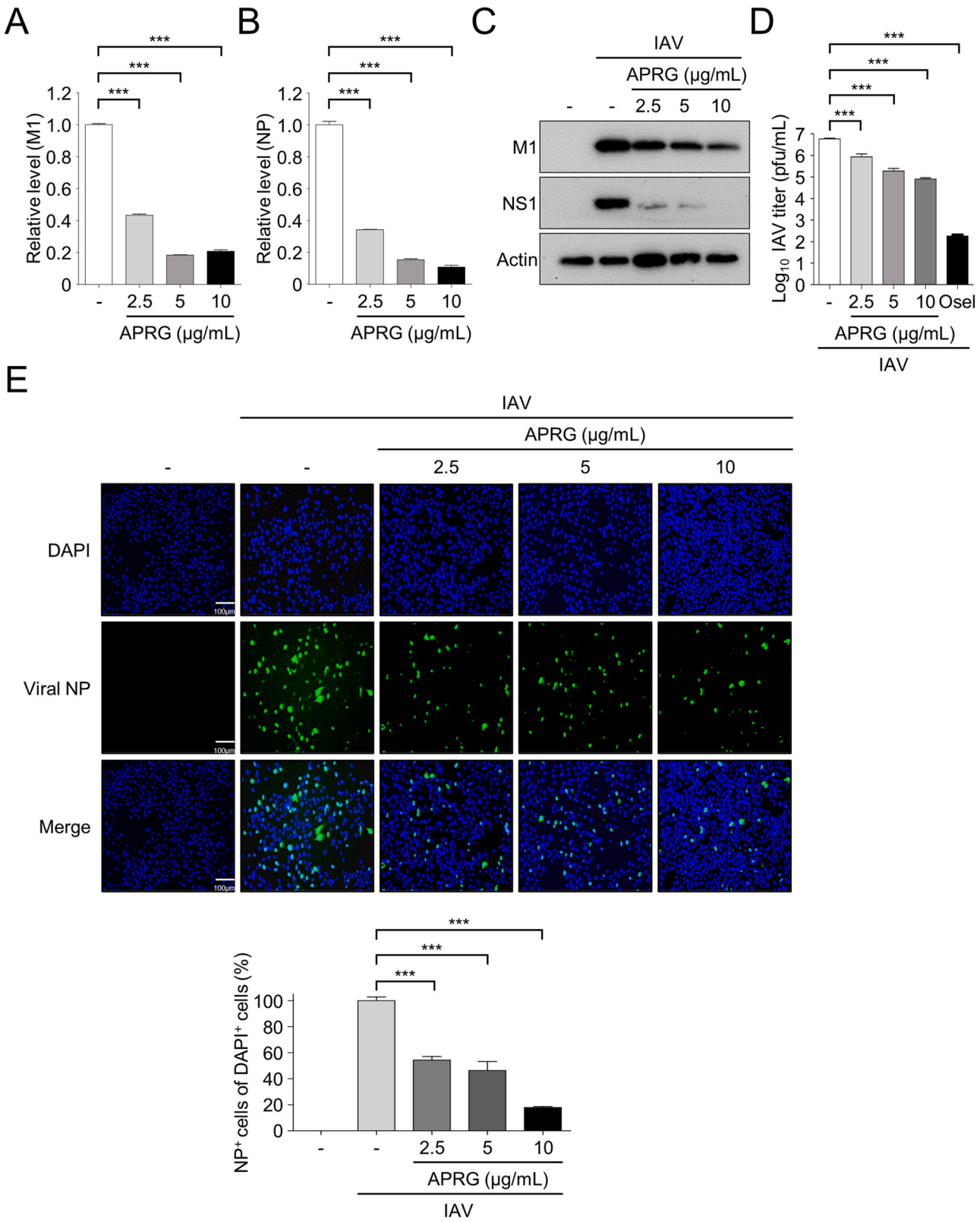

Fig. 2. The suppressive effect of APRG64 on IAV replication. (A, B) MDCK cells were infected with IAV at a multiplicity of infection (MOI) of 0.1 for 1 h and then treated with APRG64 (0, 2.5, 5 or 10 μg/mL). After 6 h, the expression level of viral M1 (A) and viral NP (B) was analyzed by RT-qPCR ($n = 3$). (C) Expression level of IAV M1 and NS1 protein was analyzed by western blot. Actin was used as a loading control. (D) MDCK cells were infected with IAV at an MOI of 0.001 for 1 h, then untreated or treated with APRG64 (2.5, 5 or 10 μg/mL) or oseltamivir phosphate (10 μg/mL) for 24 h, followed by titration of infectious viral particles using the plaque assay ($n = 3$). (E) MDCK cells were infected with IAV at an MOI of 0.1 and then treated with APRG64 (0, 2.5, 5 or 10 μg/mL) for 6 h. Viral NP proteins (green) and nuclei ($DAPI^+$, blue) were visualized by immunocytochemistry analysis ($n = 3$). Representative images (left panel) and the percentage of NP^+ cells relative to $DAPI^+$ cells are shown. Water was used as solvent control for APRG64. All graphs represent the average of three replicates. Significance was determined by Student's *t*-test. **, $p \leq 0.01$; *** , $p \leq 0.001$. APRG: APRG64; Osel: Oseltamivir phosphate.

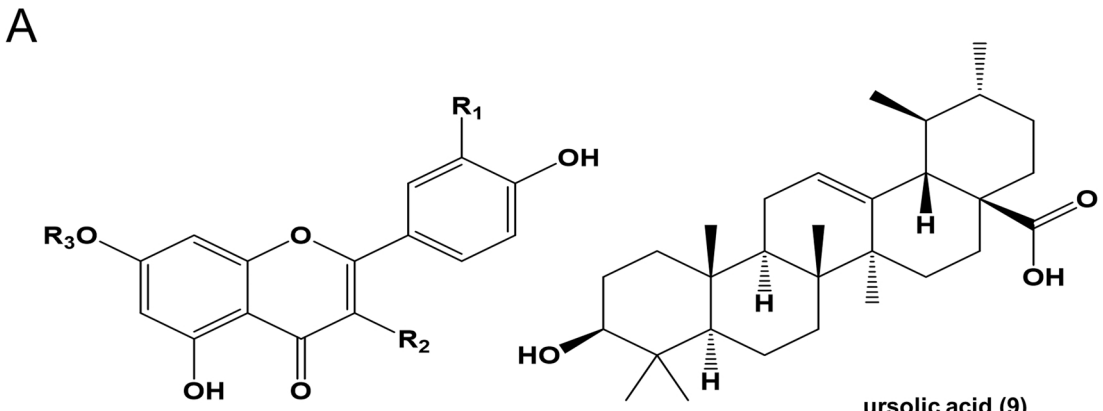

	R_1	R_2	R_3
afzelin (1)	H	rha*	H
apigenin (2)	H	H	H
apigenin 7-*O*-*β*-D-glucuronide (3)	H	H	glc**
astragalin (4)	H	glu***	H
nicotiflorin (5)	H	rut****	H
quercetin (6)	OH	OH	H
quercitrin (7)	OH	rha*	H
rutin (8)	OH	rut****	H

*α-L-rhamnopyranosyl, **β-D-glucuronosyl, ***β-D-glucopyranosyl, ****rutinosyl

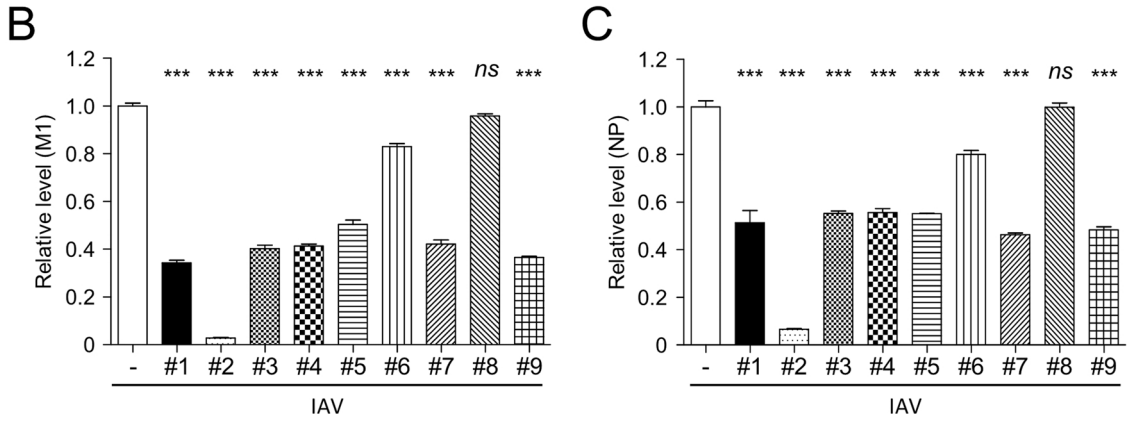

Fig. 3. Identification of anti-IAV components of APRG64. (A) Chemical structures of active components (**1**–**9**) isolated from APRG64 are shown. (**B**, **C**) MDCK cells were infected with IAV at an MOI of 0.1 for 1 h, followed by treatment with afzelin (**1**, 10 μg/mL), apigenin (**2**, 5 μg/mL), apigenin 7-*O*-glucuronide (**3**, 10 μg/mL), astragalin (**4**, 10 μg/mL), nicotiflorin (**5**, 10 μg/mL), quercetin (**6**, 2.5 μg/mL), quercitrin (**7**, 10 μg/mL), rutin (**8**, 5 μg/mL), or ursolic acid (**9**, 10 μg/mL). The relative transcription levels of viral M1 and viral NP were analyzed by RT-qPCR ($n = 3$). Significance was determined by Student's *t*-test. ns, not significant; * , $p \leq 0.05$; *** , $p \leq 0.001$.

interferon-alpha (IFN-α) for mouse, (F) 5′-GGACTTTGGATTCCCGCAGGAGAAG-3′ and (R) 5′-GCTGCATCAGACAGCCTTGCAGGTC-3′, interferon-beta (IFN-β) for mouse, (F) 5′-AACCTCACCTACAGGGCGGACTTCA-3′ and (R) 5′-TCCCACGTCAATCTTTCCTCTTGCTTT-3′, interleukin-1 alpha (IL-1α) for mouse, (F) 5′-TCTCAGATTCACAACTGTTCGTG-3′ and (R) 5′-AGAAAATGAGGTCGGTCTCACTA-3′, GAPDH for mouse, (F) 5′-TCAAGCTCATTTCCTGGTATGACA-3′ and (R) 5′-TAGGGCCTCTCTTGCTCAGT-3′. RT-qPCR was performed on a CFX Connect real-time system (Bio-Rad, Hercules, CA, USA). Each cycle threshold (C_t) was normalized to calculate ΔC_t by GAPDH. Each assay was performed at least three independent times in triplicate with similar results.

2.6. Western blot analysis

Cells were lysed using NP-40 buffer (ELPIS Biotech, Daejeon, Korea) in the presence of protease inhibitors (Thermo Scientific). Cell extracts were loaded onto a sodium dodecyl sulfate-polyacrylamide gel electrophoresis (SDS-PAGE) gel and then transferred onto a nitrocellulose membrane (GE Healthcare, Chicago, IL, USA). For blocking, the membrane was incubated with 2% BSA in TBST solution for 1 h and then incubated with a primary antibody for viral M1 (Abcam, Cambridge, UK), NP (Abcam), Actin (Santa Cruz Biotechnology, TX, USA), ERK (Cell Signaling Technology, MA, USA), p-ERK (Cell Signaling Technology), SAPK (Cell Signaling Technology), and p-SAPK (Cell Signaling Technology) overnight at 4 °C. The membrane was incubated with a secondary antibody conjugated with horseradish peroxidase (HRP; Cell

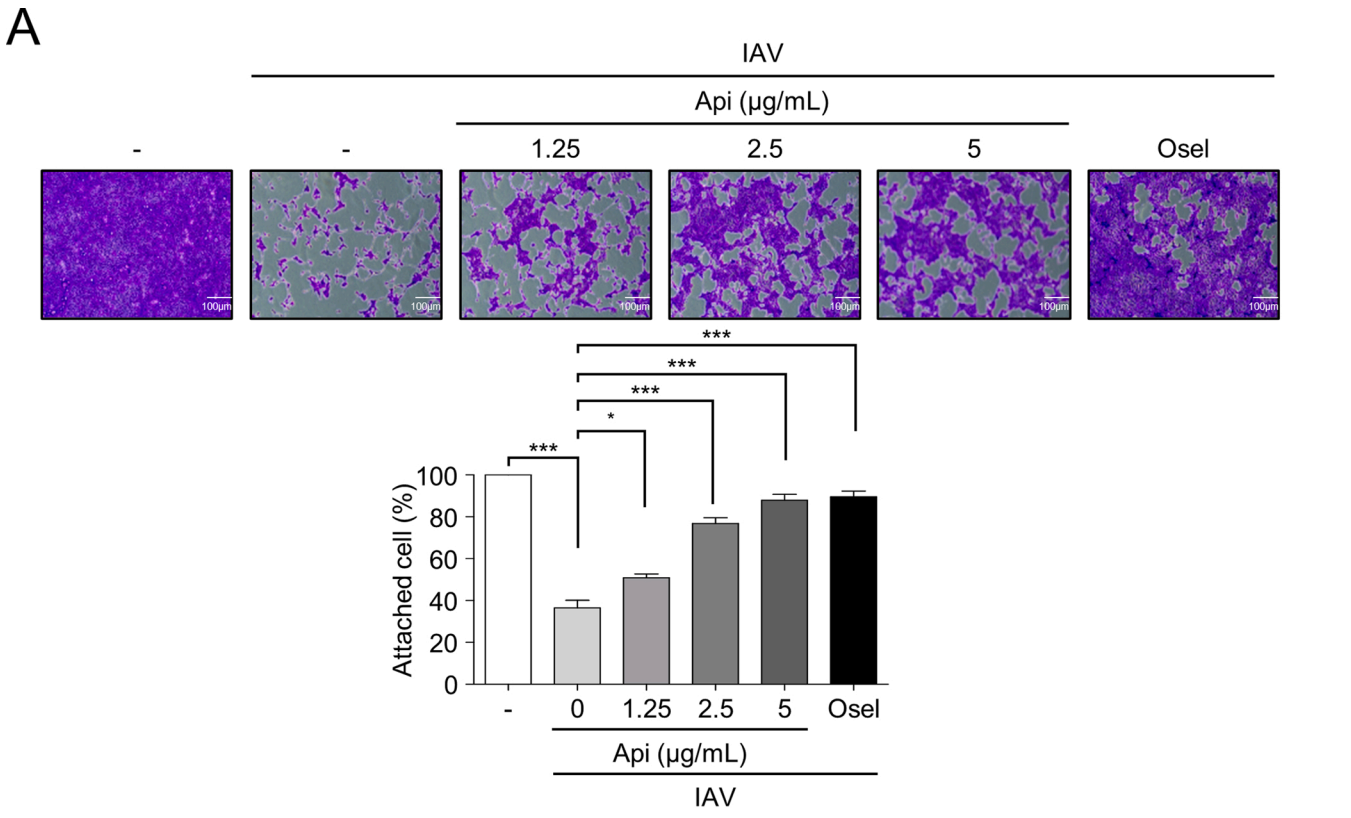

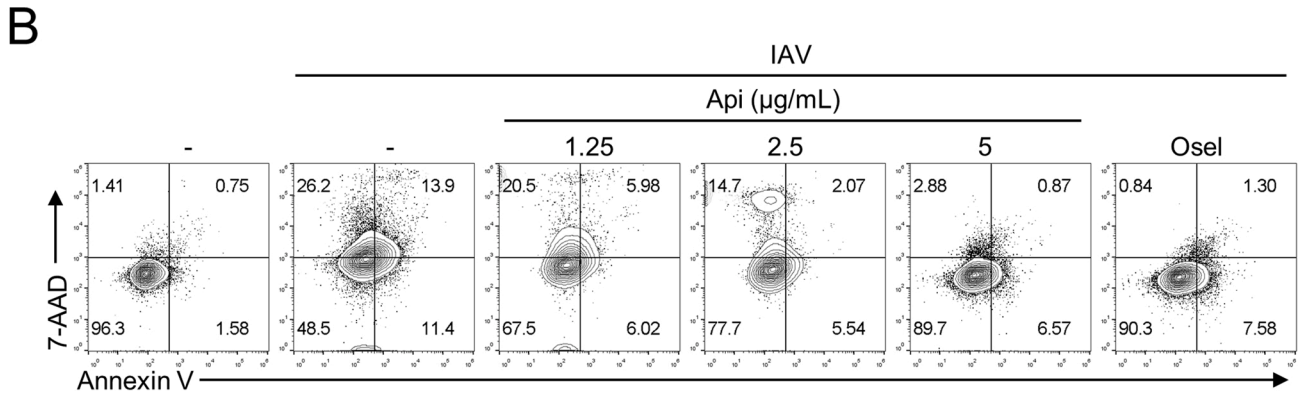

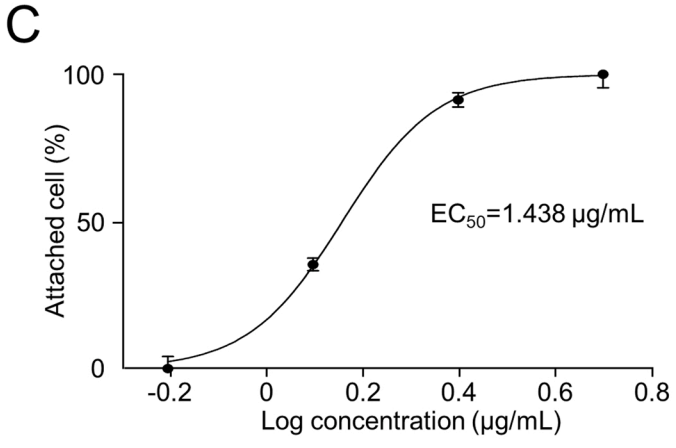

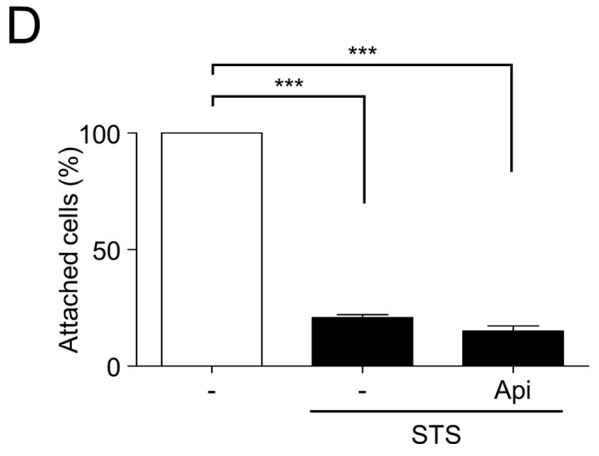

(caption on next page)

Fig. 4. Inhibitory activity of apigenin on IAV-induced CPEs. (A) MDCK cells were infected with IAV at an MOI of 0.1, then treated with or without 1.25, 2.50, or 5.00 μg/mL of apigenin or 10 μg/mL of oseltamivir phosphate. After 24 h, cells were stained with 1 % crystal violet solution to analyze attached cells. Representative images and the percentage of attached cells are shown. (**B**) MDCK cells were infected with IAV at an MOI of 0.1 for 1 h, then untreated or treated with apigenin (1.25, 2.5, or 5 μg/mL) or oseltamivir phosphate (10 μg/mL). After 12 hpi, cells that were stained with 7-AAD and Annexin V were analyzed by flow cytometry. (**C**) MDCK cells were infected with IAV at an MOI of 0.1 and then treated with apigenin (0, 0.625, 1.25, 2.50, or 5.00 μg/mL). At 24 hpi, attached cells were quantified to calculate the EC_{50} of apigenin. (**D**) MDCK cells were untreated or treated with 200 nM of staurosporine (STS) in the presence or absence of apigenin (5 μg/mL). A CPE assay was conducted to determine cell viability. Images were processed by ImageJ software to quantify attached cells on the plate. Water was used as solvent control for apigenin. All graphs represent the average of three replicates. Significance was determined by Student's *t*-test. ns, not significant; * , $p \leq 0.05$; **, $p \leq 0.01$; *** , $p \leq 0.001$. Api: Apigenin; Osel: Oseltamivir phosphate.

Signaling Technology) for 1 h at room temperature. SuperSignal West Pico PLUS Chemiluminescent Substrate (Thermo Scientific) was used to detect blotted proteins. Each assay was performed at least three independent times with similar results.

2.7. Plaque assay

The plaque assay was performed as previously described [22]. Briefly, MDCK cells were infected with IAV for 1 h, followed by incubation with MEM containing 0.3 % BSA and 0.5 % agarose (Affymetrix, Santa Clara, CA, USA) for 2 days. Cells were then fixed with 3.5 % formaldehyde and removed from the agarose gel. Plaques were visualized by staining cells with a 1% crystal violet solution.

2.8. Immunocytochemistry

MDCK cells were fixed with 4 % formaldehyde, followed by permeabilization with 0.5 % Triton X-100 (Sigma-Aldrich). After treatment with anti-IAV NP antibody (Abcam), cells were incubated with Alexa Fluor 488-conjugated secondary antibody (Thermo Scientific). DAPI (4′,6-diamidino-2-phenylindole) solution (Sigma-Aldrich) was used to detect nuclei. Cell images were captured by an N-SIM S Super Resolution Microscope (Nikon, Tokyo, Japan) and analyzed by an N-SIM image acquisition software browser (Nikon). Each assay was performed at least three independent times in triplicate with similar results.

2.9. Molecular docking analysis

The structural data of apigenin and the various viral protein including M1 (PDB ID: 4PUS), NP (PDB ID: 6J1U), NS1 effector domain (PDB ID: 3M5R), NS1 RNA-binding domain (PDB ID: 3M8A), HA receptor-binding-domain (PDB ID: 3UYW), NA (PDB ID: 6HP0), PA (PDB ID: 2ZNL), PB1 (PDB ID: 2ZNL), PB2 C-terminal domain (PDB ID: 3CW4), PB2 middle domain (PDB ID: 4J2R), and PB2 cap-binding domain (PDB ID: 4ENF) were used for molecular docking analysis. The crystal structure of proteins was retrieved from the Research Collaboratory for Structural Bioinformatics (RCSB) Protein Data Bank (PDB). Molecular docking carried out to predict binding affinity and structural conformation between apigenin and 11 viral proteins by using Autodock Vina [23] and Autodock tools 1.5.2 [24]. The structure of apigenin was converted into the PDB format using Open Babel (Ver. 2.4.1, http://openbabel.org). Subsequently, the 11 IAV proteins were imported into MGL tools (1.5.6), and polar hydrogens were added to each structure, and Kollman charges was introduced to the proteins. The ligand and IAV proteins were converted into the PDBQT (Protein Data Bank, Partial Charge (Q), and Atom Type (T)). The grid size was set to cover the entire IAV proteins with grid spacing of 1 Å. The molecular docking was performed by autodock vina with following parameters; exhaustiveness = 8, num_modes = 9, energy_range = 0.5. Five times of repeated calculation between ligand and IAV protein was performed, and the highest negative binding energy was adopted to calculate the mean binding energy and standard deviations.

2.10. Animals

All animal experiments were performed in accordance with protocols approved by the Institutional Animal Care and Use Committee at Institut Pasteur Korea (Approval No.: IPK-21,003). Six- to seven-week-old C57BL/6 male mice were used for all experiments. For oral administration, mice were intragastrically treated with 200 μL of distilled water (H_2O)-containing APRG64 (25 or 50 mg/kg) once per day. Viral RNAs, cytokines, and infectious viral particles in mouse lungs were analyzed by RT-qPCR, ELISA, or plaque assay. Each experiment was performed at least two independent times in triplicate with similar results.

2.11. Enzyme-linked immunosorbent assay (ELISA)

The mouse lung tissues were homogenized with beadbeater (Biospec Products, Bartlesville, OK, USA) in the presence of a proteinase inhibitor (Thermo Scientific). The homogenates were centrifuged at 7679 x g for 5 min at 4 °C, and the supernatant used for ELISA. To detect pulmonary TNF-α, IFN-γ, and IL-6, ELISA MAX™ Deluxe kits (BioLegend) were used according to the manufacturer's protocol. Each experiment was performed two independent times in triplicate with similar results.

2.12. Isolation procedure of active components from APRG64

The obtained extract of APRG64 (2 kg) was suspended in H_2O (1.5 L) and then successively extracted with ethyl acetate (EtOAc, 1.5 L × 3) and *n*-butanol (*n*-BuOH, 1.5 L × 3). Each layer was concentrated under reduced pressure to obtain EtOAc (APRG64-E, 178 g), *n*-BuOH (APRG64-B, 328 g), and H_2O (APRG64-W, 494 g) fractions. The APRG64-E fraction (178 g) was subjected to a SiO_2 c.c. (φ 12 × 20 cm) and eluted with chloroform−methanol ($CHCl_3$ −MeOH, 30:1→20:1→10:1→3:1; 18 L of each) to yield 25 fractions (APRG64-E-1 to APRG64-E-13). Fraction APRG64-E-13 [609.2 mg, elution volume/total volume (V_e/V_t) 0.224 − 0.230] was subjected to ODS c.c. (φ 3.5 × 5.0 cm) and eluted with acetone−H_2O (1:1→3:1; 10 L of both) to yield 17 fractions (APRG64-E-13–1 to APRG64-E-13–17). Fraction APRG64-E-13–14 (150.9 mg, $V_e/V_t = 0.315$ −0.444) was subjected to an ODS c.c. (φ 2.5 × 5.0 cm) and eluted with MeOH−H_2O (3:1; 6 L) to ultimately produce 12 fractions (APRG64-E-13–14–1 to APRG64-E-13–14–12) together with purified compound **2** [apigenin, APRG64-E-13–14–7, 10.7 mg, V_e/V_t 0.306 − 0.456, TLC (SiO_2 F_{254}) retention factor (R_f) 0.46, $CHCl_3$ −MeOH = 20:1] and compound **9** [ursolic acid, APRG64-E-13–14–10, 44.4 mg, V_e/V_t 0.621 − 0.765, TLC (SiO_2 F_{254}) R_f 0.56, $CHCl_3$ −MeOH = 20:1]. Fraction APRG64-E-23 [7.9 g, V_e/V_t 0.683 − 0.720] was subjected to an ODS c.c. (φ 7.0 × 7.0 cm) and eluted with acetone−H_2O (1:3→1:2; 30 L of both) to yield 12 fractions (APRG64-E-23–1 to APRG64-E-23–12) together with purified compound **7** [quercitrin, APRG64-E-23–5, 684.5 mg, V_e/V_t 0.423 − 0.660, TLC (SiO_2 F_{254}) R_f 0.70, $CHCl_3$ −MeOH = 2:1]. Fraction APRG64-E-23–3 (648.3 mg, V_e/V_t = 0.015 −0.023) was subjected to an ODS c.c. (φ 3.0 × 5.0 cm) and eluted with MeOH−H_2O (1:2; 8 L) to ultimately produce 11 fractions (APRG64-E-23–3–1 to APRG64-E-23–3–11) together with purified compound **6** [quercetin, APRG64-E-23–3–9, 24.1 mg, V_e/V_t 0.756 − 0.795, TLC (SiO_2 F_{254}) R_f 0.42, $CHCl_3$ −MeOH = 20:1]. Fraction APRG64-E-23–6 (258.3 mg, V_e/V_t = 0.111 −0.153) was subjected to SiO2c.c. (φ 3.0 × 15 cm) and eluted with $CHCl_3$ −MeOH−H_2O (20:3:1→10:3:1; 6 L of both) to yield 17 fractions (APRG64-E-23–6–1 to APRG64-E-23–6–17). Fraction APRG64-E-23–6–3 (81.4 mg, V_e/V_t = 0.078 −0.140) was subjected to an ODS c.c. (φ 1.5 × 8.0 cm) and eluted

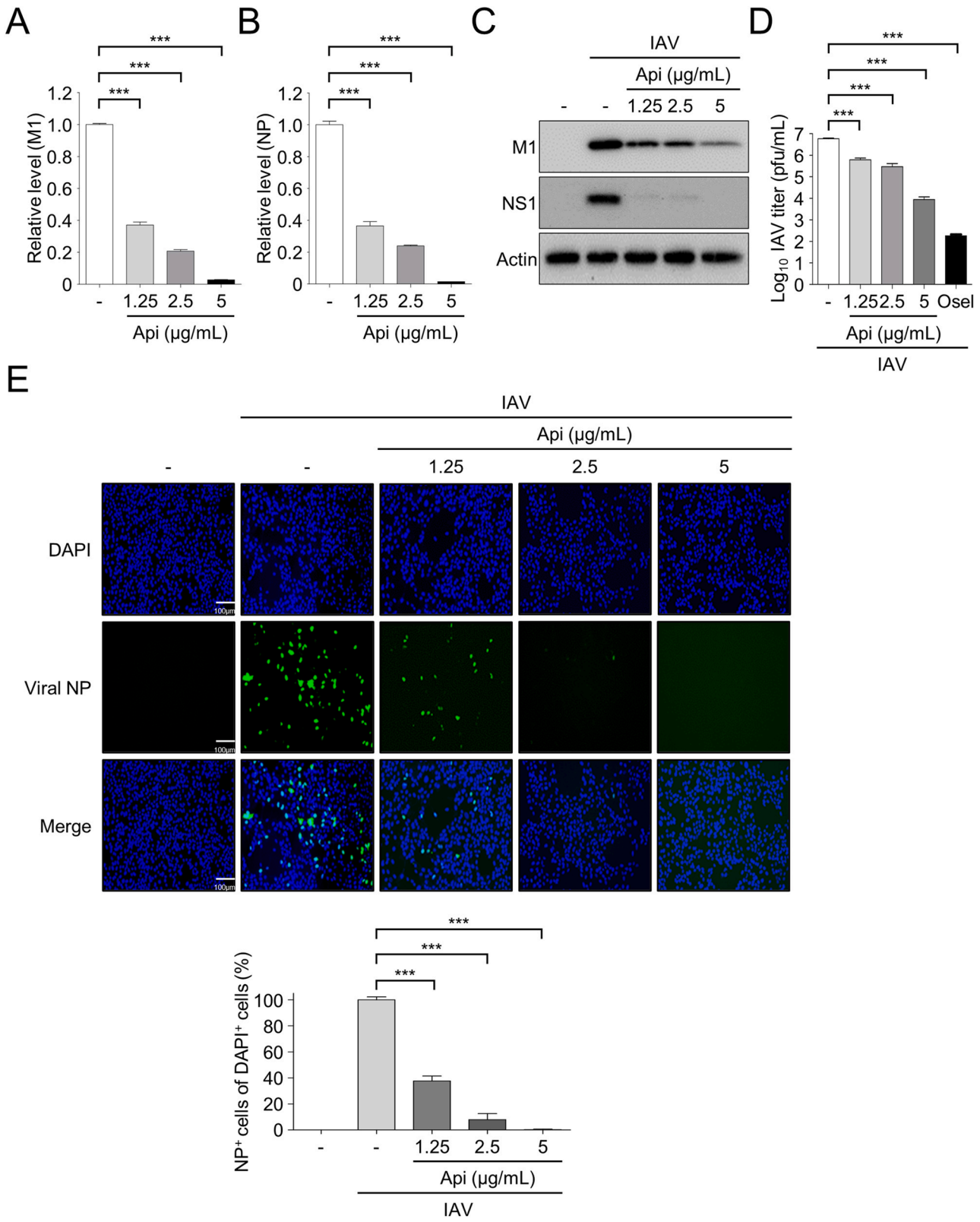

Fig. 5. The suppressive effect of apigenin on IAV replication. (A, B) MDCK cells were infected with IAV at an MOI of 0.1 for 1 h and then treated with apigenin (0, 1.25, 2.50, 5.00 μg/mL). After 6 h, the transcription level of M1 (A) and NP (B) was analyzed by RT-qPCR ($n = 3$). (C) Viral M1 and NS1 protein expression level was analyzed by western blot. Actin was used as a loading control. (D) MDCK cells were infected with IAV at an MOI of 0.001 for 1 h and then treated with apigenin (0, 1.25, 2.5, 5 μg/mL) or oseltamivir phosphate (10 μg/mL). At 24 hpi, a plaque assay was performed to measure infectious viral titers ($n = 3$). (**E**) MDCK cells were infected with IAV at an MOI of 0.1 for 1 h and then treated with apigenin (0, 1.25, 2.50, 5.00 μg/mL) for 6 h. Viral NP proteins (green) and nuclei ($DAPI^+$, blue) were visualized by immunocytochemistry analysis ($n = 3$). Representative images (left panel) and the percentage of NP^+ cells relative to $DAPI^+$ cells are shown. Water was used as solvent control for apigenin. All graphs represent the average of three replicates. Significance was determined by Student's *t*-test. *** , $p \leq 0.001$. Api: Apigenin; Osel: Oseltamivir phosphate.

Table 1
Binding energy between the 11 IAV proteins and apigenin calculated by molecular docking analysis.

IAV proteins	Apigenin
	Binding Energy (kcal / mol)
M1	-6.620 ± 0.03742
NP	-7.840 ± 0.06000
NS1_ED	-6.660 ± 0.02449
NS1_RBD	-6.760 ± 0.04000
HA_RBD	-8.280 ± 0.02000
NA	-6.700 ± 0.03162
PA	-8.000 ± 0.00000
PB1	-3.400 ± 0.00000
PB2_C terminal domain	-7.500 ± 0.00000
PB2_middle domain	-7.000 ± 0.00000
PB2_cap binding domain	-5.900 ± 0.00000

with MeOH−H_2O (2:3; 2 L) to ultimately produce eight fractions (APRG64-E-23–6–3–1 to APRG64-E-23–6–3–8) together with purified compound **1** [afzelin, APRG64-E-23–6–3–6, 6.7 mg, V_e/V_t 0.538 − 0.629, TLC (SiO_2 F_{254}) R_f 0.54, $CHCl_3$ −MeOH = 20:1]. Fraction APRG64-E-23–6–3–4 (31.8 mg, V_e/V_t = 0.156 −0.241) was subjected to a Sephadex LH-20c.c. (φ 1.5 × 50 cm) and eluted with 100% MeOH (1.5 L) to ultimately produce six fractions (APRG64-E-23–6–3–4–1 to APRG64-E-23–6–3–4–6) together with purified compound **4** [astragalin, APRG64-E-23–6–3–4–2, 26.5 mg, V_e/V_t 0.502 − 0.742, TLC (SiO_2 F_{254}) R_f 0.50, $CHCl_3$ −MeOH−H_2O = 7:3:1]. Fraction APRG64-E-23–8 (2.4 g, V_e/V_t = 0.253 −0.423) was subjected to SiO_2 c.c. (φ 4.0 × 15 cm) and eluted with $CHCl_3$ −MeOH−H_2O (20:3:1→10:3:1→7:3:1→6:4:1; 6 L of each) to ultimately produce 24 fractions (APRG64-E-23–8–1 to APRG64-E-23–8–24) together with purified compound **3** [apigenin 7-*O*-*β*-D-glucuronide, APRG64-E-23–8–3, 175.3 mg, V_e/V_t 0.056 − 0.209, TLC (SiO_2 F_{254}) R_f 0.52, $CHCl_3$ −MeOH−H_2O = 12:3:1], compound **5** [nicotiflorin, APRG64-E-23–8–5, 22.9 mg, V_e/V_t 0.377 − 0.501, TLC (SiO_2 F_{254}) R_f 0.34, $CHCl_3$ −MeOH−H_2O = 12:3:1], and compound **8** [rutin, APRG64-E-23–8–16, 7.9 mg, V_e/V_t 0.760 − 0.809, TLC (SiO_2 F_{254}) R_f 0.61, $CHCl_3$ −MeOH−H_2O = 6:4:1].

Afzelin (**1**): Yellow amorphous powder (MeOH); positive FAB/MS *m/z* 433 $[M + H]^+$; IR (KBr, *ν*) 3400, 1660, 1605, and 1500 cm^{-1}.

Apigenin (**2**): Yellow amorphous powder (MeOH); positive FAB/MS *m/z* 271 $[M + H]^+$; IR (KBr, *ν*) 3420, 2935, 1645, and 1605 cm^{-1}.

Apigenin 7-*O*-*β*-D-glucuronide (**3**): Yellow amorphous powder (MeOH); positive FAB/MS *m/z* 469 $[M + Na]^+$; IR (KBr, *ν*) 3455, 1645, 1510, and 1365 cm^{-1}.

Astragalin (**4**): Yellow amorphous powder (MeOH); positive FAB/MS *m/z* 471 $[M + Na]^+$; IR (KBr, *ν*) 3350, 2930, 2365, 1655, and 1610 cm^{-1}.

Nicotiflorin (**5**): Yellow amorphous powder (MeOH); positive FAB/MS *m/z* 639 $[M + Na]^+$; IR (KBr, *ν*) 3365, 2940, 2360, 1655, 1600, and 1515 cm^{-1}.

Quercetin (**6**): Yellow amorphous powder (MeOH); positive FAB/MS *m/z* 303 $[M + H]^+$; IR (KBr, *ν*) 3350, 1680, and 1615 cm^{-1}.

Quercitrin (**7**): Yellow amorphous powder (MeOH); positive FAB/MS *m/z* 449 $[M + H]^+$; IR (KBr, *ν*) 3358, 1659, 1610, and 1500 cm^{-1}.

Rutin (**8**): Yellow amorphous powder (MeOH); positive FAB/MS *m/z* 611 $[M + H]^+$; IR (KBr, *ν*) 3405, 3930, 1660, and 1565 cm^{-1}.

Ursolic acid (**9**): White amorphous powder (MeOH); positive FAB/MS *m/z* 457 $[M + H]^+$; IR (KBr, *ν*) 3400, 1732, and 1680 cm^{-1}.

2.13. Statistical analysis

All experiments were repeated at least twice, with similar results. Statistical significance was determined by either Student's *t*-test or Tukey's post hoc test following analysis of variance (ANOVA). Statistical analyses were conducted using Prism 5 software (GraphPad Software, Inc., La Jolla, CA, USA).

3. Results

3.1. APRG64 protects cells from IAV-induced CPE

Based on the potent antiviral activity of APRG64 against RNA viruses, such as HCV [19] and SARS-CoV-2 [20], we hypothesized that APRG64 has antiviral activity against IAV. First, we tested whether APRG64 protected cells from IAV–induced CPE. To this end, IAV (A/California/07/2009)-infected MDCK cells were treated with various concentrations (0, 2.5, 5.0, and 10 μg/mL) of APRG64 that did not induce significant cytotoxicity (Fig. S1A and S1B). While robust CPE was observed in IAV-infected, untreated MDCK cells, APRG64 treatment significantly prevented IAV–induced CPEs in a dose-dependent manner (Fig. 1A). Similarly, APRG64 was shown to prevent IAV-induced apoptosis in a dose-dependent manner (Fig. 1B). The 50 % effective concentration (EC_{50}) of APRG64 was calculated as 6.274 μg/mL (Fig. 1C). To exclude the possibility that APRG64 could prevent virus-independent cell death, MDCK cells were treated with APRG64 in the presence of staurosporine (STS), a well-known apoptosis inducer [25]. Although STS treatment potently induced cell death, additional treatment with APRG64 did not prevent STS-induced cell death (Fig. 1D). Collectively, these results suggest that APRG64 protects MDCK cells from IAV infection-induced CPEs.

3.2. APRG64 suppresses IAV replication

As CPEs occur in host cells as a result of IAV replication, the reduced CPE in APRG64-treated cells (Fig. 1) is possibly due to attenuated viral replication. To test this possibility, IAV-infected MDCK cells were treated with APRG64 and then analyzed for the production of viral mRNAs, proteins, and infectious particles. APRG64 treatment strongly suppressed the transcription of IAV M1 (Fig. 2A) and NP (Fig. 2B) in a dose dependent manner. Consistent with these results, the expression of viral proteins, including M1 and non-structural protein 1 (NS1), was substantially suppressed by APRG64 treatment (Fig. 2C). Subsequently, APRG64 treatment significantly reduced the production of infectious viral particles (Fig. 2D). Furthermore, the number of IAV NP-expressing cells was significantly reduced by APRG64 (Fig. 2E) in a dose dependent manner when analyzed by immunocytochemistry. Taken together, these results strongly support that APRG64 possesses potent anti-IAV activity.

3.3. Identification of antiviral components from APRG64

Next, we attempted to identify the active antiviral components in APRG64 responsible for its observed potent anti-IAV activity. To this end, the concentrated extracts (APRG64) were partitioned into EtOAc, *n*-BuOH, and H_2O fractions. The EtOAc fraction (APRG64-E) was used to isolate active metabolites because major flavonoid spots were observed on a TLC plate. The fractions separated by c.c. using SiO_2, ODS, and Sephadex LH-20 yielded eight flavonoids (**1**−**8**) and one triterpenoid (**9**). These compounds were identified as afzelin (**1**) [26], apigenin (**2**) [27], apigenin 7-*O*-*β*-D-glucuronide (**3**) [28], astragalin (**4**) [29], nicotiflorin (**5**) [29], quercetin (**6**) [29], quercitrin (**7**) [26], rutin (**8**) [30], and ursolic acid (**9**) [20] following extensive analysis of data from various spectroscopic methods, including IR, FAB/MS, one-dimensional ^1H, ^{13}C, and distortionless enhancement by polarization transfer (DEPT) NMR, and two-dimensional NMR experiments, specifically correlation spectroscopy (COSY), heteronuclear single-quantum correlation spectroscopy (HSQC), and heteronuclear multiple-bond correlation spectroscopy (HMBC) (Fig. 3A).

Next, we examined the anti-IAV activity of those APRG64 components. IAV-infected cells were treated with the concentration of each compound that did not significantly induce cytotoxicity (Fig. S2), followed by analyzing the transcription level of viral M1 and NP. Among the nine components, eight (afzelin, apigenin, apigenin 7-*O*-glucuronide, astragalin, nicotiflorin, quercetin, quercitrin, and ursolic acid)

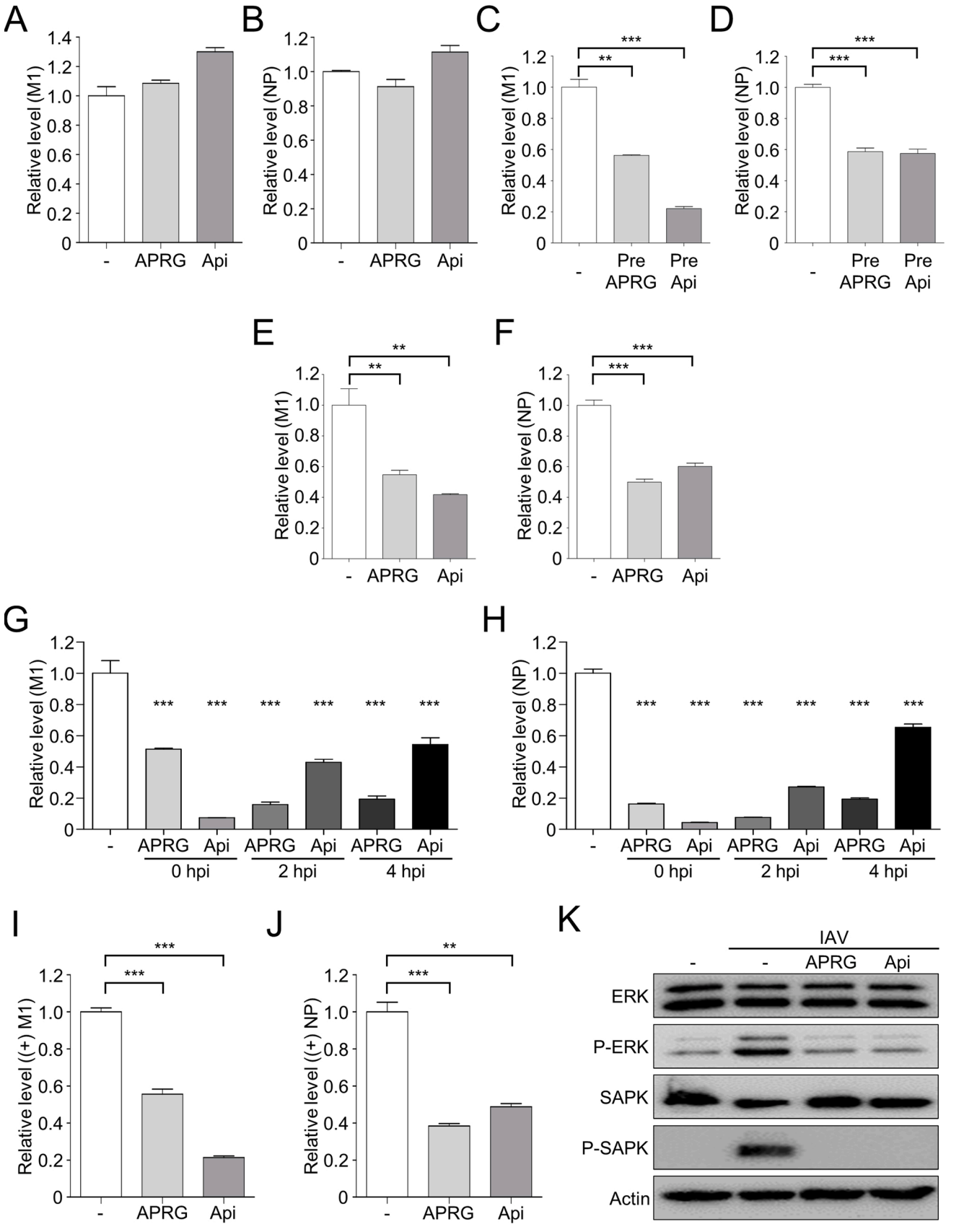

(caption on next page)

Fig. 6. The antiviral modes of action of APRG64 and apigenin. (A, B) MDCK cells were untreated or treated with 10 μg/mL of APRG64 or 5 μg/mL of apigenin for 4 h. After washing with PBS thrice, MDCK cells were infected with a 0.1 MOI of IAV for 1 h. The transcription levels of IAV M1 (**A**) and NP (**B**) were analyzed by RT-qPCR at 6 hpi ($n = 3$). (**C, D**) MDCK cells were incubated in the presence or absence of APRG64 (10 μg/mL) or apigenin (5 μg/mL) for 1 h at 37 °C and then infected with IAV for additional 1 h. At 6 hpi, the transcription levels of IAV M1 (**C**) and NP (**D**) were analyzed by RT-qPCR ($n = 3$). (**E, F**) The IAV that was incubated with 10 μg/mL of APRG64 or 5 μg/mL of apigenin for 1 h at 4 °C was added to MDCK cells. After 1 hr incubation at 37 °C, cells were washed with PBS thrice. At 6 hpi, the transcription levels of IAV M1 (**E**) and NP (**F**) were analyzed by RT-qPCR ($n = 3$). (**G, H**) MDCK cells were infected with IAV at an MOI of 0.1 for 1 h, followed by treatment with APRG64 (10 μg/mL) or apigenin (5 μg/mL) at 0, 2, or 4 hpi. At 6 hpi, the transcription levels of IAV M1 (**G**) and NP (**H**) were analyzed by RT-qPCR ($n = 3$). (**I, J**) MDCK cells were infected with IAV at a 0.1 MOI for 1 h. At 5 hpi, cells were treated with APRG64 (10 μg/mL) or apigenin (5 μg/mL). The positive (+) RNA strand expression levels of IAV M1 (**I**) and NP (**J**) were analyzed by RT-qPCR at 6 hpi ($n = 3$). (**K**) MDCK cells were infected with IAV at a 0.1 MOI for 1 h and then treated with APRG64 (10 μg/mL) or apigenin (5 μg/mL). At 6 hpi, the expression levels of ERK, p-ERK, SAPK, p-SAPK, and actin were measured by western blot. All graphs represent the average of three replicates. Water was used as solvent control for APRG64 and apigenin. Significance was determined by Student's *t*-test ± SEM. **, $p \leq 0.01$; *** , $p \leq 0.001$. APRG: APRG64; Api: Apigenin.

significantly reduced the expression of both viral M1 (Fig. 3B) and NP (Fig. 3C) mRNAs. Notably, among these components, apigenin had the most potent anti-IAV activity.

3.4. Apigenin is a major antiviral component of APRG64

Given the potent antiviral activity of apigenin, we performed additional analyses to ascertain its antiviral mode of action. When IAV-infected MDCK cells were treated with apigenin at doses (1.25, 2.50, or 5.00 μg/mL) that did not induce significant cytotoxicity (Fig. S3), IAV-induced CPEs were notably reduced in a dose-dependent manner (Fig. 4A). When cells were analyzed for apoptosis, apigenin was shown to reduce IAV-induced apoptotic cell death (Fig. 4B). Its EC_{50} was measured as 1.438 μg/mL (Fig. 4C). However, apigenin treatment did not protect cells from viral infection-independent cell death caused by STS treatment (Fig. 4D), which was similar to the protective effect of APRG64 (Fig. 1D).

Consistent with the former screening results (Figs. 3B and 3C), apigenin treatment greatly reduced the transcription (Fig. 5A and B) and expression level of viral proteins in a dose dependent manner (Fig. 5C). In addition, the production of infectious viral particles was dramatically reduced by apigenin treatment (Fig. 5D). Furthermore, when cells were treated with apigenin, viral-NP-expressing cells were barely detected (Fig. 5E), indicating its potent antiviral activity.

In order to further investigate the potential antiviral mechanism of apigenin, we conducted molecular docking analysis with respect to the IAV proteins (M1, NP, NS1 ED, NS1 RBD, HA RBD, NA, PA, PB1, PB2 C-terminal domain, PB2 middle domain, and PB2 cap-binding domain). Interestingly, apigenin has a potential to interact with viral NP (binding energy: −7.840 ± 0.06000 kal/mol), HA RBD (binding energy: −8.280 ± 0.02000 kal/mol), and polymerases (PA, binding energy: −8.000 ± 0.00000 kal/mol; PB2 C-terminal domain, binding energy: −7.500 ± 0.00000 kal/mol) with high binding energy (Table 1).

Collectively, these results indicate that apigenin is a major antiviral component of APRG64.

3.5. APRG64 and apigenin interfere with multiple steps of IAV replication

Next, we examined whether APRG64 and apigenin also have antiviral activity against other IAV strains. To this end, MDCK cells were infected with another H1N1 strain of influenza (PR8) and treated with APRG64 or apigenin. Similar to their antiviral effect on the influenza A/California/07/2009 (H1N1) strain, APRG64 and apigenin strongly decreased viral protein expression in PR8-infected cells (Fig. S4A). Furthermore, APRG64 and apigenin displayed strong antiviral activity on the influenza A/Aichi/2/68 (H3N2) (Fig. S4B). In addition, the anti-IAV activities of APRG64 and apigenin were comparable to that of oseltamivir phosphate (Tamiflu), an antiviral neuraminidase inhibitor used clinically for the treatment of IAV infection (Fig. S4C).

IAV replication begins with viral attachment, followed by viral entry into cells. Thus, we examined whether APRG64 and apigenin interfere with these early steps of viral replication. First, we tested whether APRG64 and apigenin could provide host cell protection. Cells were treated with APRG64 or apigenin for 4 h and then washed out with PBS, followed by IAV infection. However, the transcription level of viral M1 (Fig. 6A) or NP (Fig. 6B) was not significantly altered by preincubation with APRG64 or apigenin. Second, we tested whether pre-treatment with APRG64 or apigenin interferes with IAV infectivity. When cells were infected with IAV in the presence of APRG64 or apigenin, the transcription level of viral M1 (Fig. 6C) and NP (Fig. 6D) was significantly reduced. Third, we conducted virus binding assay [31] to test their effect on viral attachment. To this end, IAV that was incubated with APRG64 or apigenin 1 h was added to MDCK cells. Interestingly, APRG64 and apigenin significantly suppressed the transcription level of viral M1 (Fig. 6E) and NP (Fig. 6F). Lastly, the treatment with APRG64 or apigenin at 0, 2, or 4 h post-infection (hpi) significantly reduced viral M1 (Fig. 6G) and NP (Fig. 6H) transcription level. These results suggest that APRG64 and apigenin inhibit the early steps of IAV replication, including viral attachment and entry.

The activity of IAV RNA-dependent RNA polymerase (RdRP), which transcribes viral negative (-) RNA strands into positive (+) RNA strands, is critical for IAV replication. Therefore, we examined whether APRG64 and apigenin influence IAV RdRP activity. RdRP activity could be measured by the expression level of (+) RNA strands of IAV M1 and NP. Cells were treated with APRG64 or apigenin at 5 hpi because (+)-strands of viral M1 and NP RNAs were dramatically increased from 5 hpi [32], and their expression levels were measured. APRG64 and apigenin significantly suppressed the synthesis of the (+)-strand M1 (Fig. 6I) and NP (Fig. 6J) RNAs, indicating their potential to inhibit IAV RdRP activity. Finally, we conducted western blot analyses to test whether APRG64 and apigenin affect the activation of mitogen-activated protein kinase (MAPK) pathways, which are known to be required for IAV replication [33,34]. IAV infection dramatically induced phosphorylation of extracellular signal-regulated protein kinase (ERK) and stress-activated protein kinase (SAPK), as we expected. However, this increase was not observed in APRG64- or apigenin-treated cells (Fig. 6K). Altogether, these results demonstrate that APRG64 and apigenin inhibit multiple steps of IAV replication, including viral attachment, entry, RdRP activation, and the MAPK signaling pathway.

3.6. APRG64 and apigenin suppress IAV replication in vivo

Given the eminent antiviral activity of APRG64 and apigenin in vitro, we examined whether APRG64 and apigenin are also effective for the inhibition of IAV in vivo. To this end, mice were infected with IAV, followed by intranasal treatment with APRG64 or apigenin. Five days later, the number of infectious viral particles in the lungs was determined using a plaque assay. Consistent with the in vitro results, APRG64 (Fig. S5A) and apigenin (Fig. S5B) significantly reduced the IAV titers in the lungs. We next investigated whether oral administration of APRG64 also has an antiviral effect in mice because oral administration is the most desirable and convenient route for drug delivery. Consistent with our previous study on the safety of APRG64 [21], oral administration of APRG64 (25 or 50 mg/kg, mpk) in uninfected mice did not significantly affect the body weight (Fig. S6). However, when IAV-infected mice were treated orally with 25 or 50 mg/kg of APRG64, mice were significantly

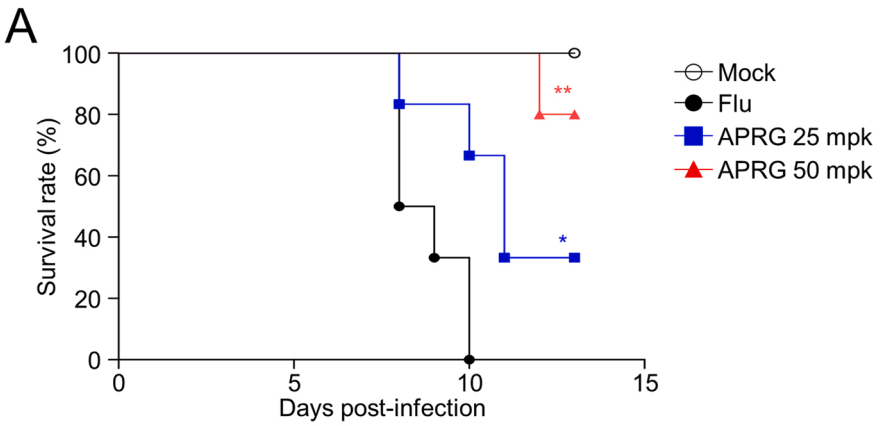

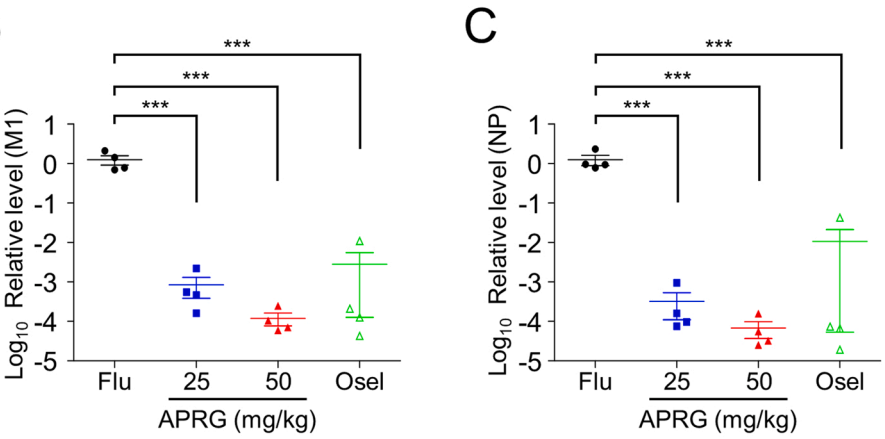

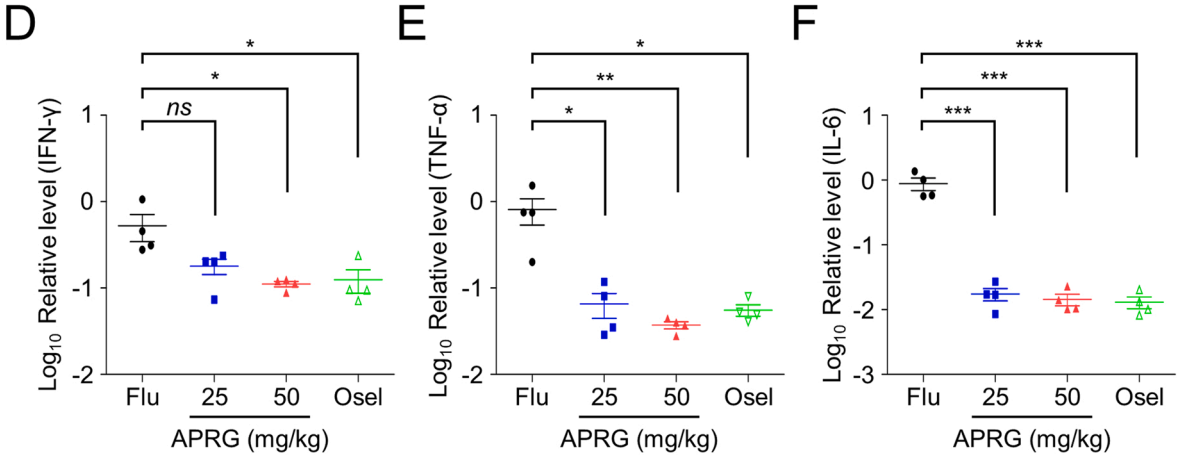

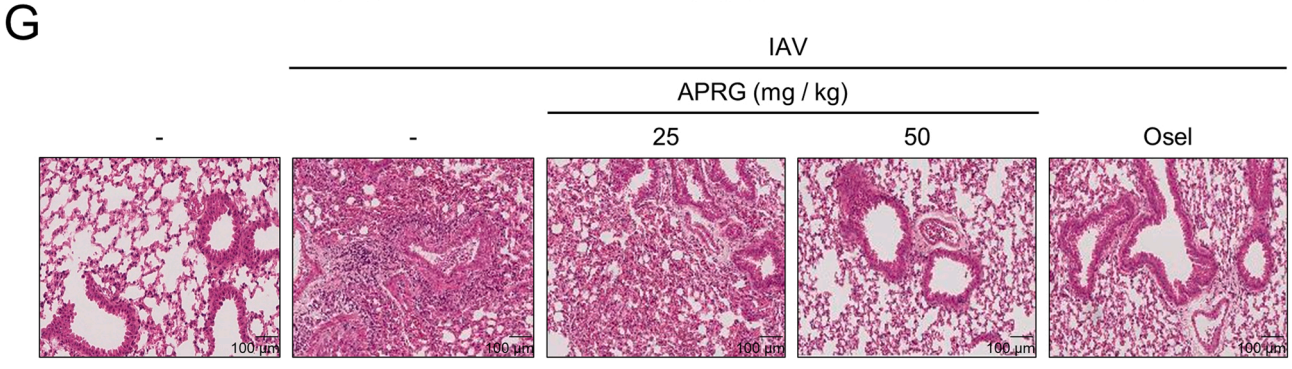

(caption on next page)

Fig. 7. The effects of APRG64 and apigenin on IAV-infected mice. (A) Wild-type C57BL/6 mice were orally administered with 0, 25, or 50 mg/kg of APRG64 for 3 days and then infected with or without 1×10^3 pfu of IAV. Oral administration of APRG64 continued for additional 5 days. Mouse survival was monitored daily for 13 days ($n = 5$). (**B-F**) Wild-type C57BL/6 mice were orally administered with 0, 25, or 50 mg/kg of APRG64 or 50 mg/kg of oseltamivir phosphate for 3 days and then infected with 1×10^3 pfu of IAV. The mice were orally administered with APRG64 or oseltamivir phosphate for an additional 5 days. At 5 dpi, mouse lungs were harvested to analyze the transcription levels of viral proteins and inflammatory cytokines. The relative transcription levels of IAV M1 (**B**), NP (**C**), IFN-γ (**D**), TNF-α (**E**), and IL-6 (**F**) were analyzed by RT-qPCR ($n = 5$). (**G**) Wild-type C57BL/6 mice were orally treated with 0, 25, or 50 mg/kg of APRG64 or 50 mg/kg of oseltamivir phosphate for 3 days and then infected with or without 1×10^3 pfu of IAV. The mice were treated with APRG64 or oseltamivir phosphate for an additional 5 days. Mice were then sacrificed to analyze lung histopathology. The representative images of hematoxylin and eosin-stained lung tissues are presented ($n = 5$). Water was used as solvent control for APRG64 and apigenin. Significance was determined by Student's *t*-test. * *, $p \leq 0.01$. APRG: APRG64; Api: Apigenin; Osel: Oseltamivir phosphate.

protected from IAV-induced mortality (Fig. 7A) in a dose-dependent manner. In addition, transcription levels of viral M1 (Fig. 7B) and NP (Fig. 7C) were significantly diminished in the lungs of APRG64-treated mice compared to those of the untreated mice at 5 dpi, which was comparable with antiviral activity of oseltamivir phosphate (Fig. 7B and C). Of note, IAV infection-induced transcription of pro-inflammatory cytokines, such as IFN-γ, TNF-α, and IL-6, in lungs was significantly suppressed by oral treatment with APRG64 (Fig. 7D–F), which was similar to the anti-inflammatory effect of oseltamivir phosphate. In addition, we observed the decreased expression of IFN-γ and TNF-α in the lungs of APRG64-treated mice when analyzed by ELISA (Fig. S7). Furthermore, the protective effects of APRG64 (25 and 50 mpk) on influenza virus-induced acute lung injury was analyzed by histopathology. The analyses using hematoxylin and eosin staining indicate that influenza virus infection-mediated immune cell infiltration into the lungs was notably decreased by APRG64 treatment in a dose dependent manner, which was comparable with the effect of oseltamivir phosphate (Fig. 7G). This protective effect of APRG64 was consistent with the reduced inflammatory cytokine level in lungs (Fig. 7D-F) and the in vitro results that APRG64 decreased the expression of pro-inflammatory cytokines in lipopolysaccharide (LPS)-stimulated splenocytes (Fig. S8). Therefore, these results collectively suggest that APRG64 could be used to treat IAV infection as a safe and effective orally administrable drug.

4. Discussion

The annual epidemic of influenza results in 3–5 million cases and up to 650,000 deaths globally [3]. Thus, it poses one of the greatest threats to public health. Plants are a source of numerous phytochemicals, such as alkaloids, flavonoids, and polyphenols, which are used as medical agents [35–38], warranting their selection for further studies for the development of medicinal plant-based antiviral therapeutics against influenza. In this study, we demonstrated the anti-IAV potential of APRG64, which is a mixture of extracts from the medicinal plants AP and RG. To identify antiviral mode of action of APRG64, we attempted to conduct several diverse experiments. Firstly, we performed cell protection assay (Fig. 6A and B), demonstrating that APRG64 does not protect cells from IAV infection. Secondly, pre-treatment experiments (Fig. 6C and D) and viral binding assays (Fig. 6E and F) suggest that APRG64 interferes with cell attachment of IAV. Thirdly, post-treatment experiments (Fig. 6G and H) reveal that APRG64 inhibits early stage of viral replication after cell attachment. Finally, we performed an experiment to test whether APRG64 affects RdRP activity (Fig. 6I and J), demonstrating that APRG64 suppresses the synthesis of the (+)-strand of viral RNAs. Thus, these results suggest that APRG64 inhibits multiple steps of IAV replication. This might allow APRG64 to be used to treat various influenza virus strains, including drug-resistant strains. In that regard, our results show that APRG64 displays potent antiviral activity against H1N1 (A/California/07/2009 and PR8) and H3N2 (A/Aichi/2/68) IAV strains. Importantly, APRG64 has already shown antiviral activities against other RNA viruses, such as HCV [19] and SARS-CoV-2 [20]. Thus, APRG64 could be used to treat a wide array of RNA viruses; however, this requires further investigation.

Among the major components in APRG64, apigenin was identified as the most potent antiviral component (Figs. 3 and 4). Apigenin is one of the flavonoids of AP and has been reported to display anti-oxidation activity [39] and anti-inflammation activity [40]. In addition, apigenin is known to prevent the development of several diseases, such as lung fibrosis [41] and liver damage [42]. Interestingly, anti-influenza viral activity of apigenin-containing herbal extracts has been reported in several previous studies. For example, the extract of *Elsholtzia rugulosa*, *Mosla scabra*, or *Geranium sanguineum L* was demonstrated to have potent anti-influenza viral activity, and apigenin was one of the major antiviral components in these extracts [43–47]. Also, Brazilian propolis (AF-08)-oriented apigenin were shown to exhibit antiviral activity against oseltamivir- and peramivir-resistant influenza viruses [48,49]. Therefore, plant extracts that contain apigenin have a great potential to be developed as antiviral phytomedicines to treat influenza virus infection.

Despite the anti-IAV activity of apigenin reported in previous studies [47,50,51], its underlying mode of action and in vivo antiviral activity have rarely been investigated. In this study, we demonstrated that apigenin interferes with viral attachment, entry, RdRP activity, and infection-induced activation of the MAPK signaling pathway (Fig. 6). Furthermore, intranasal administration of apigenin in mice strongly suppressed IAV replication (Fig. S5). Thus, apigenin could be a promising candidate for novel anti-IAV therapeutics. Our results may also lead to the development of novel apigenin derivatives with potentially more potent anti-IAV activity than apigenin.

Since apigenin, one of the main components in AP, was proved to be the most potent anti-IAV component, AP extract alone could be developed as an antiviral drug to treat IAV. This way would be more beneficial for the quality control of the herbal extract as phytomedicine than using a mixture of AP and RG. Despite this benefit of using AP extract alone, APRG64 might have potential advantages as a novel anti-IAV drug. Other components of APRG64 than apigenin such as afzelin, apigenin 7-*O*-glucuronide, astragalin, nicotiflorin, quercetin, quercitrin, and ursolic acid also displayed significant anti-IAV activity (Fig. 3). Although further investigations are required, each of these components might have a unique mode of antiviral action for IAV different from that of apigenin. Considering that broad-spectrum antiviral drugs are necessary to control newly emerged mutant viruses, APRG64 containing multiple antiviral components could be potentially effective for treating IAV variants such as drug-resistant viruses.

As an orally administrable drug, the safety of APRG64 was proved in our previous study [21]. When IAV-infected mice were orally administered with APRG64, they were significantly protected from mortality (Fig. 7 A). This could be primarily due to the potent antiviral activity of APRG64, as demonstrated in vitro (Figs. 1 and 2) and in vivo (Fig. 7). During viral infection, the exaggerated production of IFN-γ, TNF-α, and IL-6 leads to immunopathogenesis and lung injury [52,53]. Thus, the anti-inflammatory property of antiviral drugs is proposed as an important therapeutic aid that reduces symptoms and deaths by cytokine storms [54]. Interestingly, APRG64 administration strongly downregulated the expression levels of IFN-γ, TNF-α, and IL-6 in the lungs of IAV-infected mice (Fig. 7D– F), and apigenin has been reported to diminish the expression levels of TNF-α and IL-6 in LPS-stimulated macrophages [55]. Given that the production of pro-inflammatory cytokines is regulated by MAPK signaling [56–58], attenuated activation of MAPK signaling mediated by APRG64 might cause reduced

expression of pro-inflammatory cytokines. Therefore, along with the antiviral activity, the anti-inflammation activity of APRG64 could ameliorate IVA-associated symptoms and complications, contributing to the increased survival rate of IAV-infected mice.

5. Conclusions

In summary, we demonstrated that APRG64 and its main component, apigenin, have prominent antiviral effects against IAV. Their notable antiviral effect on IAV is attributed to their inhibition of multiple steps in viral replication. These in vitro antiviral effects were reproduced when APRG64 or apigenin was intranasally or orally administered to IAV-infected mice. Furthermore, oral administration of APRG64 showed strong anti-inflammation properties, which might mitigate symptoms mediated by IAV infection. Considering these results, APRG64 has great potential as a novel medication to treat IAV-infected patients.

CRediT authorship contribution statement

Yong-Hyun Joo: Methodology, Investigation, Writing – original draft, Visualization. **Yeong-Geun Lee:** Investigation, Writing – original draft, Visualization. **Younghyun Lim:** Methodology, Investigation. **Hoyeon Jeon:** Methodology, Investigation. **In-Gu Lee**: Methodology, Investigation. **Yong-Bin Cho:** Methodology, Investigation. **So-Hee Hong:** Investigation, Writing – review & editing. **Eui Ho Kim:** Methodology, Investigation. **Soon Ho Choi:** Methodology, Writing – review & editing. **Jung-Woong Kim:** Conceptualization, Writing – review & editing, Supervision. **Se Chan Kang:** Conceptualization, Writing – review & editing, Supervision. **Young-Jin Seo:** Conceptualization, Writing – review & editing, Supervision.

Conflict of interest statement

We confirm that there are no conflicts of interest associated with this publication and there has been no significant financial support for this work that could have influenced its outcome.

Data Availability

Data will be made available on request.

Acknowledgments

This research was supported by the National Research Foundation of Korea (NRF) grant funded by the Korean government [grant number NRF-2018R1A5A1025077 and 2020R1A6A3A01100042] and the Chung-Ang University Graduate Research Scholarship in 2021.

Appendix A. Supporting information

Supplementary data associated with this article can be found in the online version at doi:10.1016/j.biopha.2022.113773.

References

[1] U. Arbeitskreis Blut, Influenza virus, Transfus. Med. Hemother. 36 (1) (2009) 32–39.
[2] M. Moghadami, A narrative review of influenza: a seasonal and pandemic disease, Iran. J. Med. Sci. 42 (1) (2017) 2–13.
[3] A.E. Macias, J.E. McElhaney, S.S. Chaves, J. Nealon, M.C. Nunes, S.I. Samson, B. T. Seet, T. Weinke, H. Yu, The disease burden of influenza beyond respiratory illness, Vaccine 39 (1) (2021). A6-A14.
[4] L. Simonsen, P. Spreeuwenberg, R. Lustig, R.J. Taylor, D.M. Fleming, M. Kroneman, M.D. Van Kerkhove, A.W. Mounts, W.J. Paget, G.L.C. Teams, Global mortality estimates for the 2009 Influenza Pandemic from the GLaMOR project: a modeling study, PLoS Med. 10 (11) (2013), e1001558.
[5] M.M.G. Lorenzo, M.J. Fenton, Immunobiology of influenza vaccines, Chest 143 (2) (2013) 502–510.
[6] S.M. Kalarikkal, G.B. Jaishankar, Influenza Vaccine, StatPearls, Treasure Island (FL), 2022.
[7] P. Ryt-Hansen, A.G. Pedersen, I. Larsen, C.S. Kristensen, J.S. Krog, S. Wacheck, L. E. Larsen, Substantial antigenic drift in the hemagglutinin protein of swine influenza A viruses, Viruses 12 (2) (2020).
[8] F.G. Hayden, A.T. Pavia, Antiviral management of seasonal and pandemic influenza, J. Infect. Dis. 194 (2) (2006) S119–S126.
[9] R.A. Bright, M.-j Medina, X. Xu, G. Perez-Oronoz, T.R. Wallis, X.M. Davis, L. Povinelli, N.J. Cox, A.I. Klimov, Incidence of adamantane resistance among influenza A (H3N2) viruses isolated worldwide from 1994 to 2005: a cause for concern, Lancet 366 (9492) (2005) 1175–1181.
[10] M. Yamaki, M. Kashihara, K. Ishiguro, S. Takagi, Antimicrobial principles of Xian he cao (Agrimonia pilosa), Planta Med. 55 (2) (1989) 169–170.
[11] M.F. Hsu, J.H. Young, J.P. Wang, C.M. Teng, Effect of hsien-ho-t'sao (Agrimonia pilosa) on experimental thrombosis in mice, Am. J. Chin. Med. 15 (1–2) (1987) 43–51.
[12] K. Miyamoto, N. Kishi, R. Koshiura, Antitumor effect of agrimoniin, a tannin of Agrimonia pilosa Ledeb., on transplantable rodent tumors, Jpn. J. Pharm. 43 (2) (1987) 187–195.
[13] D.H. Kwon, H.Y. Kwon, H.J. Kim, E.J. Chang, M.B. Kim, S.K. Yoon, E.Y. Song, D. Y. Yoon, Y.H. Lee, I.S. Choi, Inhibition of hepatitis B virus by an aqueous extract of Agrimonia eupatoria L, Phytother. Res.: Int. J. Devoted Pharmacol. Toxicol. Eval. Nat. Prod. Deriv. 19 (4) (2005) 355–358.
[14] B.S. Min, Y.H. Kim, M. Tomiyama, N. Nakamura, H. Miyashiro, T. Otake, M. Hattori, Inhibitory effects of Korean plants on HIV-1 activities, Phytother. Res. 15 (6) (2001) 481–486.
[15] N.G.M. Attallah, A.H. El-Kadem, W.A. Negm, E. Elekhnawy, T.A. El-Masry, E. I. Elmongy, N. Altwaijry, A.S. Alanazi, G.A. Al-Hamoud, A.E. Ragab, Promising antiviral activity of agrimonia pilosa phytochemicals against severe acute respiratory syndrome coronavirus 2 supported with in vivo mice study, Pharmaceuticals 14 (12) (2021).
[16] W.J. Shin, K.H. Lee, M.H. Park, B.L. Seong, Broad-spectrum antiviral effect of Agrimonia pilosa extract on influenza viruses, Microbiol. Immunol. 54 (1) (2010) 11–19.
[17] J.-G. Choi, S.-H. Mun, H.S. Chahar, P. Bharaj, O.-H. Kang, S.-G. Kim, D.-W. Shin, D.-Y. Kwon, Methyl gallate from Galla rhois successfully controls clinical isolates of Salmonella infection in both in vitro and in vivo systems, PLoS One 9 (7) (2014), e102697.
[18] H.-A. Lee, S.-H. Hong, S.-J. Han, O.-J. Kim, Antimicrobial effects of the extract of Galla rhois on the long-term swine clinical trial, J. Vet. Clin. 28 (1) (2011) 1–6.
[19] J.E. Kwon, Y.G. Lee, J.H. Kang, Y.F. Bai, Y.J. Jeong, N.I. Baek, Y.J. Seo, S.C. Kang, Anti-viral activity of compounds from Agrimonia pilosa and Galla rhois extract mixture, Bioorg. Chem. 93 (2019), 103320.
[20] Y.-G. Lee, K.W. Kang, W. Hong, Y.H. Kim, J.T. Oh, D.W. Park, M. Ko, Y.-F. Bai, Y.-J. Seo, S.-M. Lee, Potent antiviral activity of Agrimonia pilosa, Galla rhois, and their components against SARS-CoV-2, Bioorg. Med. Chem. 45 (2021), 116329.
[21] J.H. Park, J.S. Ra, J.E. Kwon, Y.M. Her, T.H. Choe, Y.S. Lee, H.J. Suh, S.Y. Shin, D. W. Park, H.H. Kwak, H.M. Woo, H. Jeon, S.C. Kang, Evaluation of genetic toxicity, acute and sub-chronic oral toxicity and systemic safety of Agrimonia pilosa and Rhus gall 50% ethanolic extract mixture (APRG64) in vitro and in vivo (rodent and non-rodent animal models), Toxicol. Res. 36 (4) (2020) 367–406.
[22] Y.-J. Seo, C.J. Pritzl, M. Vijayan, K. Bomb, M.E. McClain, S. Alexander, B. Hahm, Sphingosine kinase 1 serves as a pro-viral factor by regulating viral RNA synthesis and nuclear export of viral ribonucleoprotein complex upon influenza virus infection, PLoS One 8 (8) (2013), e75005.
[23] O. Trott, A.J. Olson, AutoDock Vina: improving the speed and accuracy of docking with a new scoring function, efficient optimization, and multithreading, J. Comput. Chem. 31 (2) (2010) 455–461.
[24] C.A. Hunter, K.R. Lawson, J. Perkins, C.J. Urch, Aromatic interactions, J. Chem. Soc. Perkin Trans. 2 (5) (2001) 651–669.
[25] C.A. Belmokhtar, J. Hillion, E. Ségal-Bendirdjian, Staurosporine induces apoptosis through both caspase-dependent and caspase-independent mechanisms, Oncogene 20 (26) (2001) 3354–3362.
[26] S.W. Yun, Y.J. Seo, J.E. Kwon, D.W. Park, Y.G. Lee, T.H. Choe, S.K. Kim, H.S. Lee, H. Kim, S.C. Kang, Preclinical evaluation of Zanthoxylum piperitum Benn., traditional muscle pain remedy, for joint inflammation, J. Ethnopharmacol. 286 (2022), 114921.
[27] M.J. Kim, J.M. Han, Y.Y. Jin, N.I. Baek, M.H. Bang, H.G. Chung, M.S. Choi, K. T. Lee, D.E. Sok, T.S. Jeong, In vitro antioxidant and anti-inflammatory activities of Jaceosidin from Artemisia princeps Pampanini cv. Sajabal, Arch. Pharm. Res. 31 (4) (2008) 429–437.
[28] V. Malikov, M. Yuldashev, Phenolic compounds of plants of the Scutellaria L. genus. Distribution, structure, and properties, Chem. Nat. Compd. 38 (4) (2002) 358–406.
[29] Y.-G. Lee, H. Lee, J.-W. Jung, K.-H. Seo, D.Y. Lee, H.-G. Kim, J.-H. Ko, D.-S. Lee, N.-I. Baek, Flavonoids from Chionanthus retusus (Oleaceae) flowers and their protective effects against glutamate-induced cell toxicity in HT22cells, Int. J. Mol. Sci. 20 (14) (2019) 3517.
[30] Y.-G. Lee, Y.H. Nam, J.E. Gwag, J.-H. Ko, K.-H. Seo, D.Y. Lee, S.C. Kang, T.H. Kang, N.-I. Baek, Recovery effect of a rutin-enriched fraction prepared from forsythia koreana flowers on alloxan-induced pancreatic islets in zebrafish larvae (Danio rerio), Nat. Prod. Commun. 16 (10) (2021), 1934578×211043731.
[31] B.W. Lee, T.K.Q. Ha, H.M. Cho, J.-P. An, S.K. Kim, C.-S. Kim, E. Kim, W.K. Oh, Antiviral activity of furanocoumarins isolated from Angelica dahurica against influenza a viruses H1N1 and H9N2, J. Ethnopharmacol. 259 (2020), 112945.

[32] Y.H. Joo, Y.G. Lee, Y. Lim, H. Jeon, E.H. Kim, J. Choi, W. Hong, H. Jeon, M. Ahrweiler, H. Kim, S.C. Kang, Y.J. Seo, Potent antiviral activity of the extract of Elaeocarpus sylvestris against influenza A virus in vitro and in vivo, Phytomedicine 97 (2022), 153892.
[33] R. Kumar, N. Khandelwal, R. Thachamvally, B.N. Tripathi, S. Barua, S.K. Kashyap, S. Maherchandani, N. Kumar, Role of MAPK/MNK1 signaling in virus replication, Virus Res. 253 (2018) 48–61.
[34] W. Nacken, D. Anhlan, E.R. Hrincius, A. Mostafa, T. Wolff, A. Sadewasser, S. Pleschka, C. Ehrhardt, S. Ludwig, Activation of c-jun N-terminal kinase upon influenza A virus (IAV) infection is independent of pathogen-related receptors but dependent on amino acid sequence variations of IAV NS1, J. Virol. 88 (16) (2014) 8843–8852.
[35] S. Ben-Shabat, L. Yarmolinsky, D. Porat, A. Dahan, Antiviral effect of phytochemicals from medicinal plants: applications and drug delivery strategies, Drug Deliv. Transl. Res 10 (2) (2020) 354–367.
[36] D.I. Kim, Y.B. Cho, Y. Lim, S.H. Hong, B. Hahm, S.M. Lee, S.C. Kang, Y.J. Seo, Chios mastic gum inhibits influenza A virus replication and viral pathogenicity, J. Gen. Virol. 102 (3) (2021).
[37] D. Rajasekaran, E.A. Palombo, T. Chia Yeo, D. Lim Siok Ley, C. Lee Tu, F. Malherbe, L. Grollo, Identification of traditional medicinal plant extracts with novel anti-influenza activity, PLoS One 8 (11) (2013), e79293.
[38] M. Shoji, S.Y. Woo, A. Masuda, N.N. Win, H. Ngwe, E. Takahashi, H. Kido, H. Morita, T. Ito, T. Kuzuhara, Anti-influenza virus activity of extracts from the stems of Jatropha multifida Linn. collected in Myanmar, BMC Complement. Altern. Med. 17 (1) (2017) 96.
[39] J.Y. Han, S.Y. Ahn, C.S. Kim, S.K. Yoo, S.K. Kim, H.C. Kim, J.T. Hong, K.W. Oh, Protection of apigenin against kainate-induced excitotoxicity by anti-oxidative effects, Biol. Pharm. Bull. 35 (9) (2012) 1440–1446.
[40] S. Duarte, D. Arango, A. Parihar, P. Hamel, R. Yasmeen, A.I. Doseff, Apigenin protects endothelial cells from lipopolysaccharide (LPS)-induced inflammation by decreasing caspase-3 activation and modulating mitochondrial function, Int J. Mol. Sci. 14 (9) (2013) 17664–17679.
[41] X. Zhou, T. Gao, X.-G. Jiang, M.-L. Xie, Protective effect of apigenin on bleomycin-induced pulmonary fibrosis in mice by increments of lung antioxidant ability and PPARγ expression, J. Funct. Foods 24 (2016) 382–389.
[42] R.-J. Zhou, H. Ye, F. Wang, J.-L. Wang, M.-L. Xie, Apigenin inhibits d-galactosamine/LPS-induced liver injury through upregulation of hepatic Nrf-2 and PPARγ expressions in mice, Biochem. Biophys. Res. Commun. 493 (1) (2017) 625–630.
[43] A. Pantev, S. Ivancheva, L. Staneva, J. Serkedjieva, Biologically active constituents of a polyphenol extract from Geranium sanguineum L. with anti-influenza activity, Z. für Naturforsch. C. 61 (7–8) (2006) 508–516.
[44] W. Cai, S.L. Zhang, Anti-inflammatory mechanisms of total flavonoids from mosla scabra against influenza A virus-induced pneumonia by integrating network pharmacology and experimental verification, Evid. Based Complement. Altern. Med. 2022 (2022) 2154485.
[45] Q. Wu, C. Yu, Y. Yan, J. Chen, C. Zhang, X. Wen, Antiviral flavonoids from Mosla scabra, Fitoterapia 81 (5) (2010) 429–433.
[46] C. Yu, Y. Yan, X. Wu, B. Zhang, W. Wang, Q. Wu, Anti-influenza virus effects of the aqueous extract from Mosla scabra, J. Ethnopharmacol. 127 (2) (2010) 280–285.
[47] A.-L. Liu, B. Liu, H.-L. Qin, S.M.Y. Lee, Y.-T. Wang, G.-H. Du, Anti-influenza virus activities of flavonoids from the medicinal plant Elsholtzia rugulosa, Planta Med. 74 (08) (2008) 847–851.
[48] H. Kai, M. Obuchi, H. Yoshida, W. Watanabe, S. Tsutsumi, Y.K. Park, K. Matsuno, K. Yasukawa, M. Kurokawa, In vitro and in vivo anti-influenza virus activities of flavonoids and related compounds as components of Brazilian propolis (AF-08), J. Funct. Foods 8 (2014) 214–223.
[49] T. Shimizu, A. Hino, A. Tsutsumi, Y.K. Park, W. Watanabe, M. Kurokawa, Anti-influenza virus activity of propolis in vitro and its efficacy against influenza infection in mice, Antivir. Chem. Chemother. 19 (1) (2008) 7–13.
[50] X. Xu, J. Miao, Q. Shao, Y. Gao, L. Hong, Apigenin suppresses influenza A virus-induced RIG-I activation and viral replication, J. Med. Virol. (2020).
[51] L. Xu, W. Jiang, H. Jia, L. Zheng, J. Xing, A. Liu, G. Du, Discovery of multitarget-directed ligands against influenza a virus from compound yizhihao through a predictive system for compound-protein interactions, Front. Cell. Infect. Microbiol. 10 (2020) 16.
[52] L.P. Tavares, M.M. Teixeira, C.C. Garcia, The inflammatory response triggered by Influenza virus: a two edged sword, Inflamm. Res. 66 (4) (2017) 283–302.
[53] T. Schmit, K. Guo, J.K. Tripathi, Z. Wang, B. McGregor, M. Klomp, G. Ambigapathy, R. Mathur, J. Hur, M. Pichichero, Interferon-γ promotes monocyte-mediated lung injury during influenza infection, Cell Rep. 38 (9) (2022), 110456.
[54] I. Ramos, A. Fernandez-Sesma, Modulating the innate immune response to influenza A virus: potential therapeutic use of anti-inflammatory drugs, Front. Immunol. 6 (2015) 361.
[55] X. Zhang, G. Wang, E.C. Gurley, H. Zhou, Flavonoid apigenin inhibits lipopolysaccharide-induced inflammatory response through multiple mechanisms in macrophages, PLoS One 9 (9) (2014), e107072.
[56] M.X. Lim, C.W. Png, C.Y. Tay, J.D. Teo, H. Jiao, N. Lehming, K.S. Tan, Y. Zhang, Differential regulation of proinflammatory cytokine expression by mitogen-activated protein kinases in macrophages in response to intestinal parasite infection, Infect. Immun. 82 (11) (2014) 4789–4801.
[57] A.P. de Souza, V.L. Vale, C. Silva Mda, I.B. Araujo, S.C. Trindade, L.F. de Moura-Costa, G.C. Rodrigues, T.S. Sales, H.A. dos Santos, P.C. de Carvalho-Filho, M.G. de Oliveira-Neto, R.E. Schaer, R. Meyer, MAPK involvement in cytokine production in response to Corynebacterium pseudotuberculosis infection, BMC Microbiol 14 (2014) 230.
[58] Z. Manzoor, Y.-S. Koh, Mitogen-activated protein kinases in inflammation, J. Bacteriol. Virol. 42 (3) (2012) 189–195.